Article

Immunity

TCR origin and specificity to environmental or self-antigens on distinct antigen-presenting cells determine peripheral Treg cell differentiation

Graphical abstract

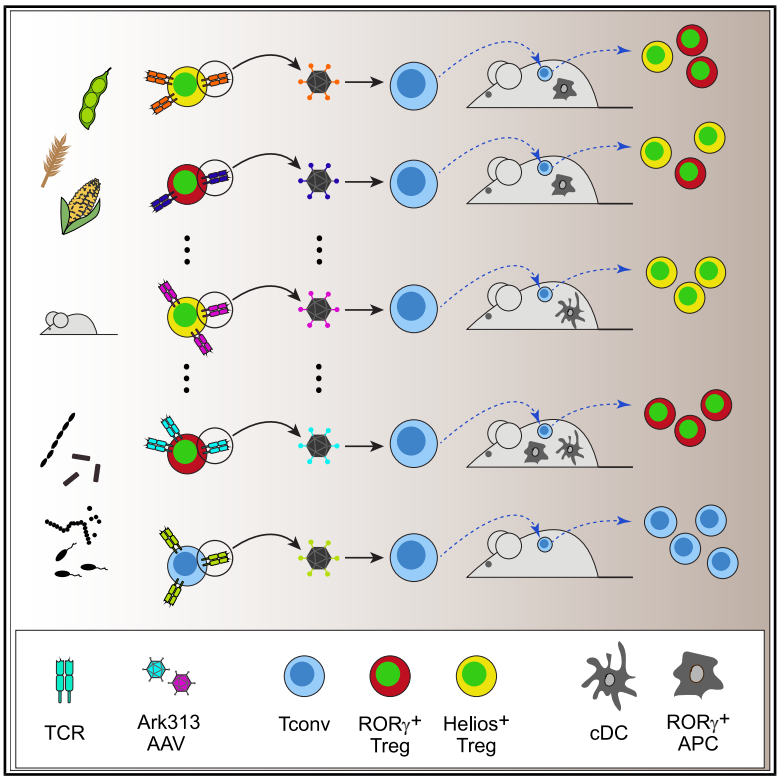

Authors

Xinxin Chi, Charlotte H. Wang, Yollanda Franco Parisotto, ..., Justin Eyquem, Chrysothemis C. Brown, Christophe Benoist

Correspondence

cbdm@hms.harvard.edu

In brief

Using CRISPR-based TCR editing, Chi et al. systematically compare gut TCRs recognizing dietary, microbial, and self-antigens to define the principles that govern peripheral Treg cell differentiation. They find that TCR identity encodes pTreg cell generation, phenotype, and antigen-presenting cell dependence, establishing TCR specificity as a primary organizer of peripheral immune tolerance.

Highlights

- CRISPR-based TCR editing of a panel of dietary-, microbial-, and self-reactive gut TCRs
- TCR identity encodes T cell fate; Treg cell-derived TCRs drive pTreg cell differentiation
- TCR-antigen pairs program distinct pTreg cell phenotypes and transcriptomes
- Involvement of different APCs for pTreg cell differentiation according to antigen source

Chi et al., 2026, Immunity *59*, 2266–2281
August 11, 2026
https://doi.org/10.1016/j.immuni.2026.07.001

CellPress

CellPress
OPEN ACCESS

Immunity

Article

TCR origin and specificity to environmental or self-antigens on distinct antigen-presenting cells determine peripheral Treg cell differentiation

Xinxin Chi,[1] Charlotte H. Wang,[2] Yollanda Franco Parisotto,[3] William A. Nyberg,[2] Vanja Cabric,[3,4] Adelaide Gelineau,[1] Yi Cao,[1] David L. Owen,[1] Jonas Ambjörnsson,[1] Diane Mathis,[1] Justin Eyquem,[2] Chrysothemis C. Brown,[3,4,5] and Christophe Benoist[1,6,*]

[1]Department of Immunology, Harvard Medical School, Boston, MA, USA
[2]Department of Medicine, University of California, San Francisco, San Francisco, CA, USA
[3]Immuno-Oncology Program, Memorial Sloan Kettering Cancer Center, New York, NY, USA
[4]Department of Pediatrics, Memorial Sloan Kettering Cancer Center, New York, NY, USA
[5]Immunology and Microbial Pathogenesis Program, Weill Cornell Medicine Graduate School of Medical Sciences, New York, NY, USA
[6]Lead contact
*Correspondence: cbdm@hms.harvard.edu
https://doi.org/10.1016/j.immuni.2026.07.001

SUMMARY

Peripheral differentiation of regulatory T (pTreg) cells promotes immunological tolerance to obligate non-self, such as food or symbiotic microbes. We examined the relative importance of TCR recognition vs. environmental cues, leveraging CRISPR-based TCR editing of primary T cells with a large TCR panel, assessing pTreg cell differentiation induced by self-, microbial, or dietary antigens. All antigen classes drove stable pTreg cell differentiation, which varied with TCR origin: TCRs derived from Treg cells enabled pTreg cell differentiation more effectively than those from conventional T cells. TCRs recognizing self-, microbial, or dietary antigens elicited distinct pTreg cell phenotypes: Helios$^+$, RORγ^+, or both. Different TCR-antigen pairs established distinct transcriptional programs. These differences traced to the types of antigen-presenting cells (APCs) involved—food-reactive TCRs depended predominantly on RORγ^+ APCs and self-reactive TCRs depended on conventional dendritic cells. Thus, TCR specificity is a primary determinant of CD4$^+$ T cell fate and phenotype, integrating antigen specificity and presentation context, providing a framework to design TCR-based tolerogenic immunotherapies.

INTRODUCTION

The gastrointestinal tract represents a unique and complex immunological environment, constantly interacting with a diverse array of dietary antigens, commensal microbes, and self-antigens. Maintaining immune homeostasis in this dynamic setting relies on appropriate immune responses to microbes and food antigens in the context of their broad communities.[1,2] CD4$^+$ T cells play a central role in these processes, and different microbes have been shown to elicit distinct responses.[3–8] Among those, regulatory T (Treg) cells that express the transcription factor FoxP3 are essential for suppressing excessive inflammation and fostering tolerance in the gut.[1,9]

Many Treg cells differentiate in the thymus (tTreg cells), driven by recognition of self-antigens, but another pool differentiates in peripheral lymphoid organs (pTreg cells) from conventional CD4$^+$ T cells (Tconv cells), a conversion driven by foreign antigens, in particular from food and microbes in the gut.[9,10] These two populations have fundamentally different operational logics, since one is focused on self-antigens initially encountered in the thymus, while the other mostly deals with foreign antigens. Accordingly, tTreg and pTreg cells play complementary parts in immunoregulation.[11–14] Understanding what drives T cells toward effector or pTreg cell differentiation is key to elucidating peripheral immune tolerance and to manipulate T cell responses for cell therapy and vaccination.

In gut-associated lymphoid tissues (GALTs), the different flavors of Treg cells can schematically be categorized into Helios$^+$ (also Gata3$^+$) and RORγ^+ (also cMaf$^+$) categories of Treg cells, as well as Helios$^-$RORγ^- double-negatives (DNs). RORγ^+ Treg cells are strongly tuned by gut bacteria.[6,15–18] They control intestinal inflammation, IgA production, and food allergies[6,13,15,19,20] and are only partially dependent on FoxP3.[13,21] In contrast, Helios$^+$ Treg cells strictly require FoxP3 and are thought to partake in tissue repair via their production of amphiregulin[22–25] but also curtail inflammation more generally. Dietary proteins have been reported to regulate DN Treg cells in small intestine.[26] It was originally thought that Helios$^+$ Treg cells are tTreg cells that differentiate in the thymus, while RORγ^+ Treg cells are pTreg cells that

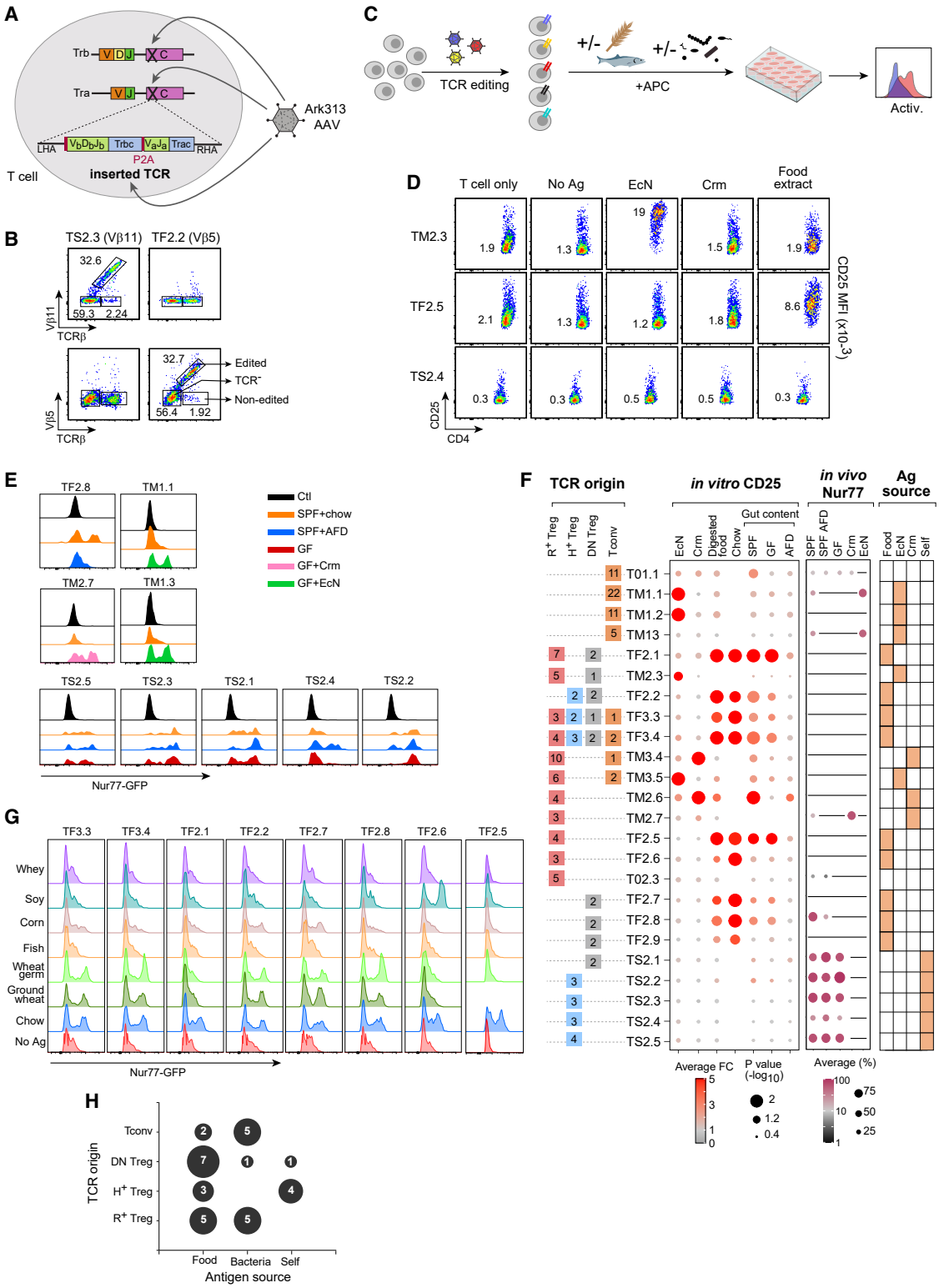

Figure 1. Reactivity of TCRs derived from colonic Treg and Tconv cells

(A) Diagram illustrating TCR editing with the Ark313 AAV vector. The AAV encodes 2 single gRNAs to cut into the C regions of TCRα and TCRβ loci, as well as an expression cassette for the TCRα and TCRβ of interest (connected by a 2A linker) that inserts by homologous recombination into the cleaved TCRα region.

(B) Representative flow cytometric plots showing TCRVβ11 and TCRVβ5 expression in CD4$^+$ T cells edited to express TS2.3 (Vβ11$^+$) or TF2.2 (Vβ5$^+$) TCRs.

(legend continued on next page)

differentiate from Tconv cells in the periphery. Transfer and lineage tracing experiments in several systems supported this notion.[13,17,27,28] On the other hand, some pTreg cells can be Helios$^+$,[28] and analyses of TCR sequencing data revealed clonotypes shared by RORγ$^+$ and Helios$^+$ Treg cells,[28,29] which implies that they share some common origin. These are not compatible with a strict Helios$^+$ = tTreg, RORγ$^+$ = pTreg equivalency, and this important question remains unresolved.

The functional importance of pTreg cells in balancing effector T cell responses to the same foreign antigens is well understood, but it is unclear what determines the conversion of a Tconv cell into a pTreg cell.[9] Are the effects of microbiota and diet on gut Treg cells direct (antigen dependent) or indirect (via metabolites and other cells)? The question is made more complex by the diversity of actors that influence colonic Treg cells: microbes have a strong influence, as do antigen-presenting cells (APCs) and, in particular, the recently described RORγ$^+$ APCs.[30–32] Neuroimmune connections are involved, and we showed that Trpv1$^+$ sensory neurons modulate RORγ$^+$ Treg cells.[7,33,34] The characteristics of the antigens that can drive pTreg cell generation are also unclear. Is it simply a matter of a cell being activated by a strong agonist in peripheral tissues? If so, any Tconv cell should have the ability to become a pTreg cell. Another model posits that more specific cues, encoded in its TCR, determine a T cell's ability to become a pTreg cell—for instance, by signaling with a particular intensity range or by recognizing antigen presented by a particular type of APC.

These questions have been difficult to address because of the limited range of TCRs that can be explored with transgenic models. Individual transgenic models support pTreg cell generation with variable efficacy,[17,35] but it is unclear how to generalize from one-off observations. Recent work from our lab analyzed in detail the phenotypes and TCRs of colonic CD4$^+$ T cells in mice colonized by single microbes, identifying thousands of individual clonotypes.[29] Some of these were shared between colonic Treg and Tconv cells, suggesting involvement in pTreg cells. Here, by leveraging this data store and a powerful system for efficient TCR engineering in primary mouse T cells, we performed a mini-screen to assess the ability of a diverse panel of TCRs to drive pTreg cell differentiation. The results reveal that all TCRs are not equal. The ability to become a pTreg cell, and to adopt the RORγ$^+$ phenotype, are both deeply predetermined by a cell's TCR, by the class of antigen that it recognizes, and by the type of APC that presents it.

RESULTS

Colonic CD4 TCRs are activated by food, bacterial, and self-antigens

To understand the potential of TCRs from colonic CD4 in shaping cell destiny, we selected from our previous dataset[29] a panel of 24 clonal expanded TCRs derived from CD4$^+$ T cells isolated from colonic lamina propria of gnotobiotic mice monocolonized with *Clostridium ramosum or Escherichia coli* Nissle. These TCRs encompass a range of representations of several cell-types (Tconv cells, Treg cells of different phenotypes [RORγ$^+$, Helios$^+$, or RORγ$^-$Helios$^-$ (DN)]) (Figure S1). To functionally express these TCRs in normal T cells, we utilized a CRISPR-Cas9-based TCR knockin system recently established by some of us.[36] This system utilizes the adeno-associated virus (AAV) variant Ark313, evolved to infect primary mouse T cells. It delivers to cells from Cas9-expressing transgenic mice, in a single vector, guide RNAs (gRNAs) that inactivate endogenous *Trac* and *Trbc* loci and a template for homology-directed repair targeting *Trac* that inserts the sequences coding for the TCR of interest under the control of the endogenous promoter (as a 2A-spaced bicistronic construct; Figure 1A). The endogenous *Trac* and *Trbc* genes are inactivated in ~90% of transduced primary CD4$^+$ T cells, 20%–40% of which express the desired TCR, detectable by the appropriate TCR-V-specific monoclonal antibodies (illustrated for two such constructs in Figure 1B; note that the process leaves in the cultures a few T cells non-edited cells, as well as TCR$^-$ cells, which provided useful internal standards in the experiments below).

To assess the antigen specificity of the TCR panel, we co-cultured TCR-edited CD4$^+$ splenocytes with APCs loaded with different complex antigens: heat-killed bacteria, protein extract from colon content, solubilized mouse chow, intestinal content (from SPF or germfree mice, fed standard chow or a protein-antigen-free [amino acid based diet, hereafter antigen-free diet (AFD)]) (Figure 1C). CD25 induction was used as an indicator of responses (Figure 1D; Table S1). Specific reactivity to microbial (*E. coli* Nissle or *C. ramosum*) or food antigens was readily identified in this manner for 15 of the 24 TCRs tested, including TCRs emanating from Tconv or various Treg cell subsets (Figure 1D, tabulated in Figure 1F), indicating that colonic CD4$^+$ T cells include a very high frequency of T cells reactive to gut luminal antigens. In contrast to a previous report,[37] we did not detect polyreactive T cells that respond to antigens from several microbes,

(C) Schematic experimental design: CD4$^+$ T cells are edited to express different TCRs and cultured with APCs supplemented with different sources of intestinal antigens before readout of activation markers by flow cytometry.
(D) Flow cytometric plots of CD25 expression in TCR-edited cells co-cultured with the indicated antigens, representative of 2 or more experiments. Numbers are mean fluorescence intensity (MFI). EcN: *E.coli* Nissle; Crm: *C. ramosum*.
(E) Representative experiment: CD4$^+$ T cells from Nur77-GFP/Cas9 mice were TCR-edited and transferred into the indicated hosts. After 24 h, mesenteric lymph nodes (mLNs, gated on donor-derived edited cells) were analyzed for activation denoted by GFP expression. "Ctl" controls were TCR$^-$ cells from those transfers.
(F) Summary of the characteristics and reactivity of all TCRs used in this study. From left to right: summary of the type of colonic CD4$^+$ T cell in which the TCRs were originally discovered,[29] with numbers of cells expressing these clonotypes; compilation of the *in vitro* CD25 induction experiments, dot plot displaying average fold change (FC), and −log10 (*p* value) of CD25 MFI relative to APC-only controls; compilation of *in vivo* Nur77-GFP$^+$ induction experiments, as % GFP$^+$ cells among TCR-edited cells; black line: not done; a summary of the antigen specificity for all TCRs used in this study. *p* values were determined using a one-sample *t* test.
(G) TCR-edited Nur77-GFP/Cas9 CD4$^+$ were co-cultured with APC and protein extracts for 6 h; plots of GFP expression are representative of 2 or more experiments.
(H) Summary plot connecting the TCRs' antigen specificity with their cell type of origin (dots sized according to the number of instances; clonotypes found in several cell types counted more than once).

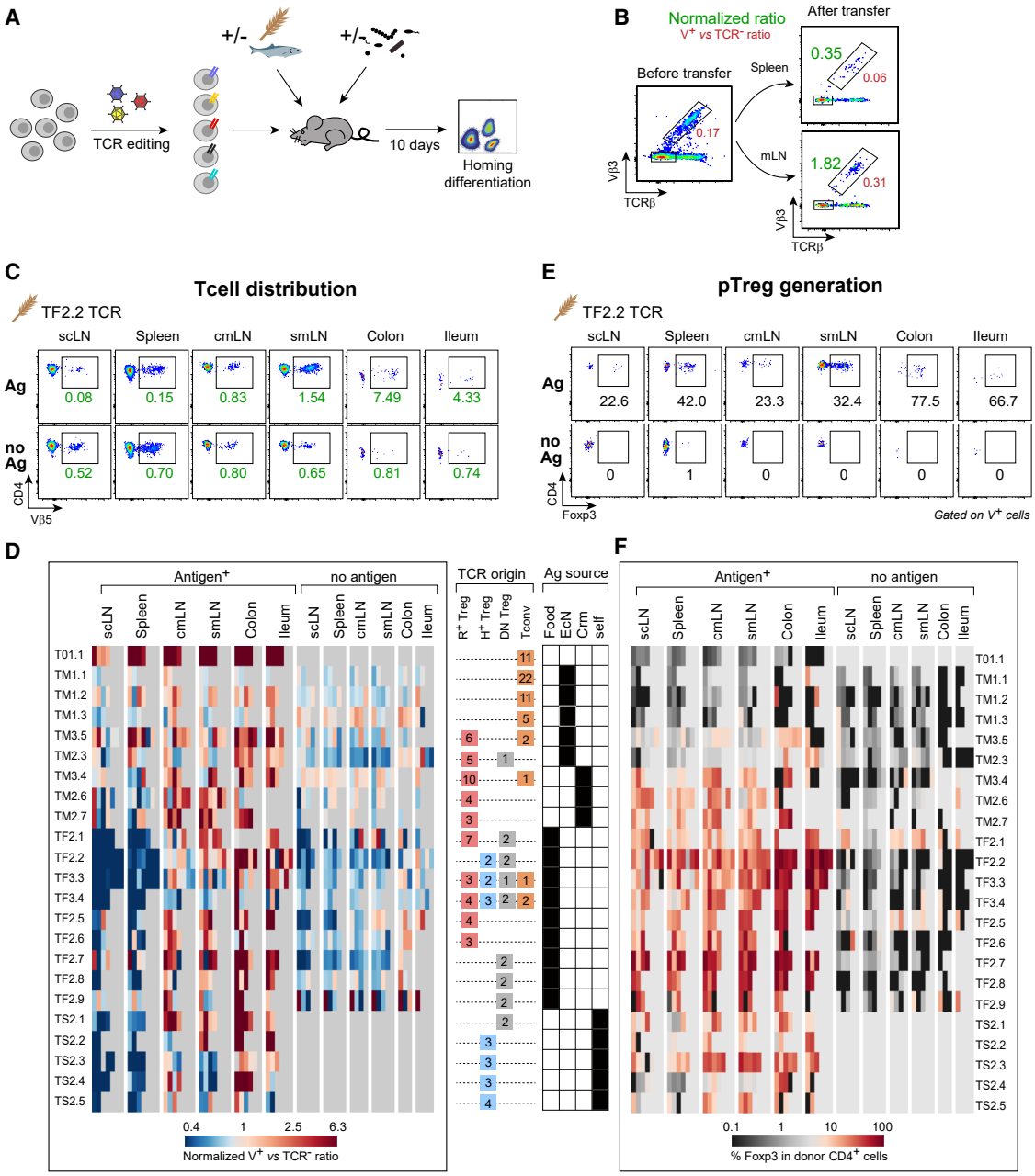

Figure 2. TCR-antigen recognition directs T cell tissue distribution and pTreg cell generation

(A) Diagram of experimental design: CD4$^+$ Tconv cells were TCR-edited as above and transferred into host mice, which provided, or not, the corresponding antigen sources. For food antigens: SPF mice fed regular chow or AFD diet; for microbial antigens: SPF mice gavaged or not with *E. coli* Nissle, or germ-free mice gavaged or not with *C. ramosum*; for self-reactive TCRs: SPF mice, no controls possible. Donor-derived cells in different tissues were analyzed 10 days after transfer.

(B) Representative plots depicting the normalization method used. After editing to express the TF2.8 TCR (Vβ3$^+$), the donor cell population was normalized to TCR$^-$ cells in each pool (red numbers; note how it increased in the mLN relative to spleen), and their relative abundance in each organ was further normalized to before-transfer values (green numbers) to enable comparison across different experiments.

(C) Representative flow cytometric plots of tissue distribution of TF2.2-expressing cells in different organs, 10 days after transfer (scLN, subcutaneous LN; cmLN, colon-draining LN; smLN, SI-draining LN) green numbers: normalized representation in each tissue, calculated as detailed in (B).

(D) Compilation of tissue distribution of all transfer experiments as in (C), representing the normalized ratio of TCR-edited cells (V$^+$) vs. TCR$^-$ cells across different tissues. Results in recipients devoid of antigen (A) are shown at right. Each bar an individual host, $n = 3$–6, with a few dropouts because cell numbers were too low for quantitation. A recall from Figure 1 of TCR origin and specificity is shown at right.

(E) Representative flow cytometric plots of FoxP3 expression in TF2.2-expressing cells, 10 days after transfer.

(legend continued on next page)

but this may result from different microbiota (community vs. monocolonized) in mice from which the TCRs emanated.

This simple *in vitro* activation system might miss reactivities to some antigens that would require processing and presentation by APCs *in vivo*. We set an *in vivo* test system wherein the TCRs whose antigen specificity could not be determined *in vitro* were edited into T cells from Nur77-GFP reporter mice, in which GFP expression denotes TCR stimulation.[38,39] Confirming *in vitro* results, cells expressing the food-reactive TF2.8 TCR upregulated Nur77-GFP expression in normal but not AFD-fed hosts, and cells expressing the TM1.1 TCR were activated in *E. coli* Nissle-colonized but not in SPF hosts (Figures 1E and 1F), In this assay, five TCRs (TS2.1–TS2.5) that seemed unresponsive *in vitro* proved to be activated *in vivo* in all hosts, irrespective of microbe (germ free [GF]) or food antigens (AFD), indicating responsiveness to self-antigens rather than bacterial or dietary antigens (Figures 1E and 1F; Table S1). No antigen reactivity could be identified for T02.3 and T01.1 TCRs. Thus, by combining *in vitro* co-culture and *in vivo* assays, we identified 8 microbe-reactive, 9 food-reactive, and 5 self-reactive TCRs (Figure 1F).

Although we did not aim here to formally identify the actual peptides recognized by these food-reactive TCRs, it was of interest to assess whether they corresponded to a single protein type or immunodominant epitope. Hence, we cultured TCR-edited Nur77-GFP reporter cells with APCs and extracts from specific components of normal mouse chow, which identified several different patterns: reactivity to soy extract for 1 TCR; to wheat for 5 other TCRs, of which 2 cross-reacted with corn; and the specific antigen source of 2 was not identified (Figure 1G). Thus, the TCRs in our panel that react to dietary antigens recognize a variety of epitopes, although dominated by grain proteins, a diversity comparable to that recently reported.[40]

Integrating these response data showed that the types of colon T cells from which these TCRs originate was clearly related to their specificity (Figure 1F) as further summarized in Figure 1H. Self-reactive TCRs mostly originated only from Helios$^+$ Treg cells. Microbe-reactive TCRs stemmed from either Tconv or RORγ^+ Treg cells, consistent with the types of cells known to be microbe-reactive.[6,20,41–44] Food-reactive TCRs derived from the broadest array of colonic cells, including Tconv and all Treg cell subsets, arguing for a broad phenotypic dispersion of the immune response to food antigens.

TCR-antigen recognition directs T cell fate and tissue distribution

Having decoded the categories of antigens that activated the panel of colon TCRs, we then asked how TCRs reactive to different antigens would drive the differentiation of CD4$^+$ Tconv cells (clonal proliferation or pTreg cell generation?). Congenically-marked (Thy1.1) spleen Tconv cells were edited as above to express individual TCRs from our panel, their FoxP3-negative status verified (Figure S2A), and transferred into normal host mice in which the cognate antigens were present or absent (Figure 2A; for food-specific TCRs, mice fed regular chow vs. AFD diet; for microbe-specific TCRs, SPF or GF mice colonized or not with *E. coli* Nissle or *C. ramosum*). To streamline this screen, cells expressing different TCRs were often multiplexed for transfer into the same host (Figure S2B), which also enhanced the comparability between different TCRs. Thy1.1$^+$ donor cells were identifiable 10 days later in different locations, in systemic lymphoid organs (spleen and subcutaneous lymph nodes [scLNs]) and in GALTs (small intestine-draining LNs [smLNs], colon-draining mesenteric LNs [cmLNs], colon, and ileum lamina propria [LP]; Figure S2C). For quantitation, we normalized their numbers to those of the co-transferred TCR$^-$ cells (and relative to this ratio at the time of transfer) to reflect cognate TCR-driven cell accumulation in each tissue (Figure 2B). Representative results for one TCR are shown in Figure 2C, but several important findings emerged from the fully integrated results (23 TCRs in 155 independent transfers, Figure 2D and Table S2). First, irrespective of specificity (food, microbe, or self), virtually all of these TCRs drove preferential accumulation in GALT locations and a relative depletion in systemic lymphoid organs. This accumulation was antigen-dependent, largely disappearing in Ag-free control hosts. The exceptions were T01.1, which induced a run-away expansion in all tissues, and TM3.5, which showed comparable enrichment in all tissues. Second, different TCRs led to preferential distribution in the intestinal tissues themselves (colon, ileum, TF2.2, and TS2.2) or in the draining LNs (TM2.6 and TF2.6; Figure 2D). Moreover, individual TCRs displayed organ-preferential patterns. For example, TF2.1-expressing cells preferentially accumulated in the ileum and its draining smLNs, whereas TS2.4-expressing cells were more enriched in the colon and its draining cmLNs.

We then examined the capacity of individual TCR-antigen pairs to direct pTreg cell differentiation in the same transfers. As illustrated in Figure 2E for the TF2.2 TCR, FoxP3$^+$ pTreg cells were detected abundantly 10 days after transfer, not only in GALTs but also in systemic lymphoid organs. pTreg cell differentiation was completely abrogated in the absence of antigen (Figure 2E, bottom row). The full data (Figure 2F; Table S2) confirmed this dependency. Furthermore, essentially none of the co-transferred TCR$^-$ or non-edited cells developed FoxP3 expression (Figure S2D), showing that a TCR-dependent trigger was required. There was, however, substantial variation in the ability of different TCRs to support pTreg cell differentiation, as illustrated in Figure 2F, which reveals several trends. First, TCRs originally identified exclusively in Tconv cells (T01.1, TM1.1, TM1.2, and TM1.3, top rows in Figure 2F) generally failed to induce Treg cells, no matter in monocolonized gnotobiotic mice or SPF mice gavaged with *E. coli* Nissle following streptomycin treatment (TM1.1 and TM1.2 in Figure S2E), while all those originally from Treg cells did so, if to varying extents. Second, TCRs that recognize food antigens generally promoted pTreg cells more robustly than those reactive against microbial or self-antigens—a trend observed in both *E. coli* Nissle

(F) Compilation of FoxP3 expression in donor cells (as in E) for all transfer experiments, in antigen-positive or negative hosts, color-coded as the percent FoxP3$^+$ cells among Edited$^+$CD4$^+$ T cells. Each bar represents an individual mouse (n = 3–6). Only samples with more than 10 cells for each TCR-edited population were included in the analysis shown in (D) and (F).

monocolonized mice and SPF mice (Figure S2E). Third, more pTreg cell differentiation was observed with TCRs reactive against *C. ramosum* than against *E. coli* Nissle, in keeping with *C. ramosum* being one of the strongest Treg cell inducers in our previous monocolonization studies.[6] Finally, varying the number of input Tconv cells over a 5-fold range did not markedly affect the resulting pTreg cell proportions (Figure S2F), suggesting that pTreg cell conversion is not strongly limited by niche sizes.

TCRs originally derived from colonic Treg cells reactive against self-antigens drove pTreg cell differentiation with a preferential tissue localization in the GALT (Figure 2F), which seemed paradoxical given that self-reactive Treg cells are usually thought to originate in the thymus. To rule out reactivity against a food or microbial antigen that would have escaped our earlier assays, we transferred edited Tconv cells into hosts devoid of microbial (germfree), or dietary (AFD), or both (AFD-fed germfree) sources of foreign antigens. Except for TS2.5, pTreg cell generation was comparable in all hosts, confirming that true self-reactivity is involved (Figure S2G). These results suggest that reactivity against self-antigens, apparently gut-specific but unrelated to dietary or microbial antigens, is able to drive pTreg cell differentiation.

pTreg cells are generally considered to be specific to mucosal tissues, and it was surprising to find them disseminated in so many locations. Although lower in proportion, pTreg cells in the spleen do form large contingents (roughly 25% of the pTreg cells generated in any one mouse are found in the spleen [Figures 2E and 2F]). To rule out that these splenic pTreg cells might be due to the particular conditions of our Cas9/AAV editing system, we performed parallel transfers with Tconv cells from two lines of transgenic mice (BθOM and HH7-2) that express TCRs reactive against antigens from *Bacteroides thetaiotaomicron* and *Helicobacter hepaticus*, respectively.[8,17] As with the transfer of TCR-edited cells above, pTreg cells from these transgenically encoded TCRs were detected in various tissues, including the spleen and scLNs but only in microbe-carrying hosts (Figure S2H), ruling out a quirk of the TCR editing system. HH7-2tg TCR transgenic cells exhibited higher pTreg cell generation than BθOM cells, reflecting again the differential ability of TCR/antigen/APC combinations to support pTreg cell generation.

To determine where pTreg cells first appear, we traced their generation over time. For food- and self-antigen-reactive TCRs, pTreg cell formation was first observed in the mesenteric lymph nodes (mLNs) as early as 2 days post-transfer, conversion of cells expressing microbe-reactive TCRs exhibiting a slower response (Figures S3A and S3B). pTreg cells only accumulated a little later in the spleen. Together with the data above, we interpret these kinetics to mean that differentiation first occurs in the mLNs, with secondary spread to the spleen or to intestinal tissues, a balance controlled in part by availability of antigen in different locales.

Collectively, these findings suggest that pTreg cells can be induced by food, bacteria, or self-antigens, widely distributed in hosts and are not restricted to gut-associated tissues.

pTreg cell phenotypes are determined by the TCR

As introduced above, colonic Treg cells exist in functionally different phenotypes (RORγ$^+$, Helios$^+$, or DN), and the relationship between these phenotypes and Treg cell origin (pTreg and tTreg cells) is debated. We thus leveraged our panel of TCRs to assess the phenotypes adopted by pTreg cells elicited by individual TCR-antigen pairs after transfer of edited cells into antigen-carrying hosts. Several important observations stood out. First, pTreg cells generated by antigen-driven conversion from transferred Tconv cells can adopt several different phenotypes: predominantly Helios$^+$ for TS2.3 (albeit with slightly lower levels of Helios expression than in host's Treg cells, Figure S4), predominantly RORγ$^+$ for TM2.7, both for TF2.2 (Figure 3A). All pTreg cells also included a strong contingent of DNs. These results clearly established that pTreg cells are not obligatorily RORγ$^+$. Second, these phenotypes correlated strongly with the class of antigen recognized by the TCRs. Microbes predominantly induced RORγ$^+$ pTreg cells in the mLNs, as also visible in colon and spleen (Figure 3B), while self-reactive pTreg cells exclusively expressed Helios, with no RORγ expression detected in any tissue. In contrast, dietary antigens induced pTreg cells exhibit a mixed phenotype, expressing either RORγ or Helios in the mLNs or spleen, with a shift to higher RORγ expression pattern in colon (Figures 3A and 3B). These results, integrated in Figure 3C, indicate that pTreg cell phenotype is shaped by the TCR-antigen pair and suggest further molding by the colon microenvironment. Third, as explicitly shown in Figure 3D, the phenotype adopted by the pTreg cells was also strongly conditioned by the phenotype of the cell from which we originally isolated the αβTCR: RORγ$^+$ pTreg cells were mostly induced by TCRs originally isolated from RORγ$^+$ pTreg cells. This link again supports the notion that the TCR encodes, likely by the antigen specificity, the nature of the APCs that present this antigen, the environment in which activation occurs, and the phenotype of the resulting pTreg cells.

In normal mice, RORγ$^+$ Treg cells are highly represented in the colonic LP, relative to mLNs and other tissues, and their proportions are modulated by microbes, as shown by gnotobiotic and antibiotic experiments.[6,15] We thus asked whether microbes would alter the proportion of RORγ$^+$ pTreg cells, even for cells whose differentiation was driven by a food antigen. We compared RORγ$^+$ frequencies among pTreg cells expressing the food-reactive TF2.2 TCR, after transfer in hosts carrying different microbiota: normal complex microbiota (SPF), single microbe (monocolonized with *E. coli* Nissle or *C. ramosum*), or none (germfree; Figure 3E). The distribution of pTreg cell phenotypes, high RORγ$^+$ in colon and high Helios$^+$ in spleen remained consistent in these conditions (Figure 3E). Thus, food antigens can drive the differentiation of RORγ$^+$ pTreg cells, without requiring contributions from gut microbes.

Several studies from our group and others have found that IL-6,[6,15,28,33] including IL-6 derived from neurons,[46] plays an important role in tuning the population of RORγ$^+$ Treg cells in the colon, but it was unclear whether this reflected an influence on pTreg cell differentiation or on a homeostatic setpoint. To address this question, we implemented a sequential editing strategy of primary Tconv cells, first inactivating the *Il6ra* locus by electroporation of Cas9/gRNA complexes,[45] prior to TCR editing as above. We then transferred these cells, as an internally controlled co-transfer of TF2.2 or TF2.5-edited Tconv cells,

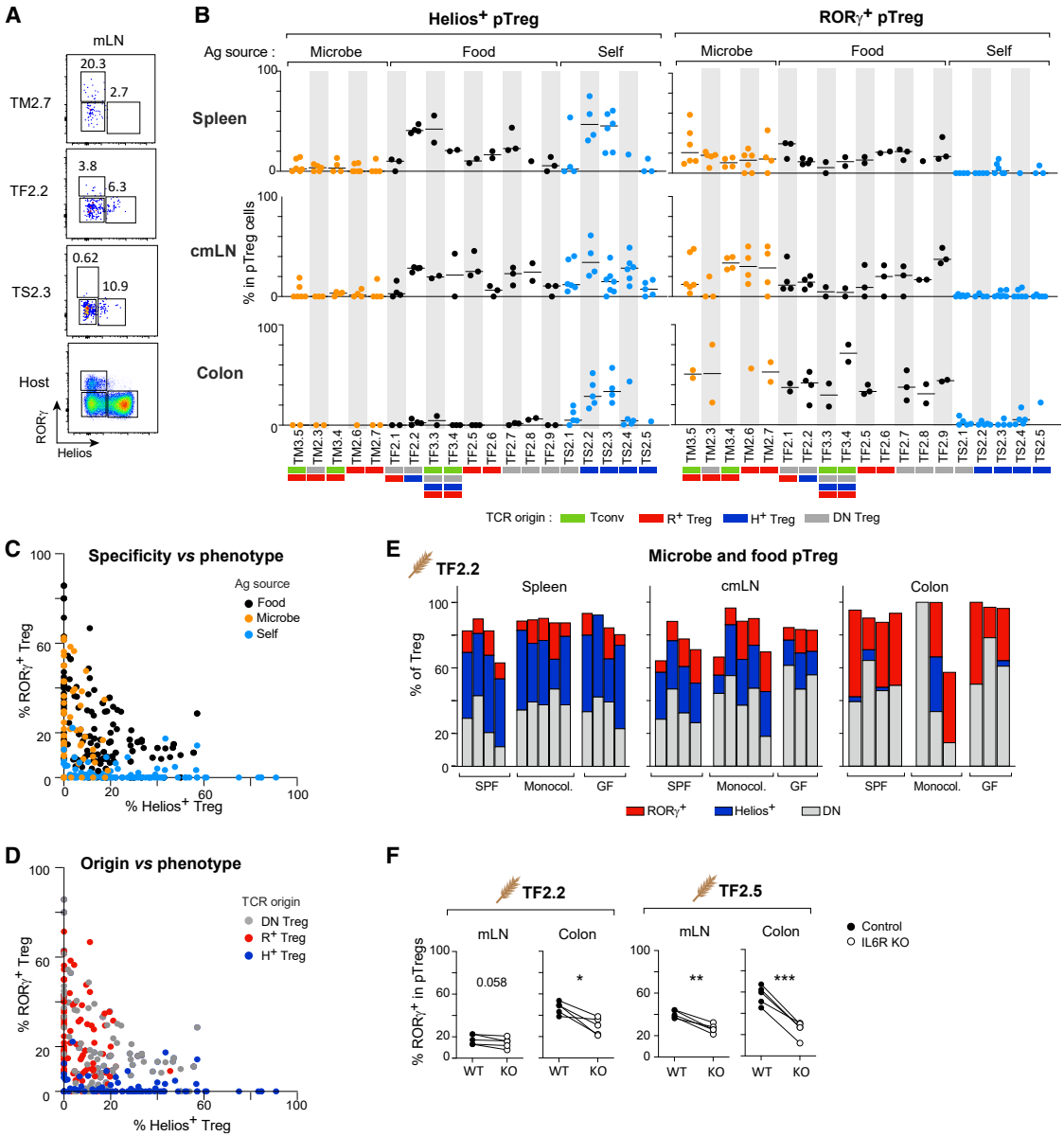

Figure 3. pTreg cells can adopt either RORγ vs. Helios phenotypes, driven by TCR specificity and origin

(A) Representative plots showing RORγ vs. Helios expression patterns in TCR-edited pTreg cells in mLN (day 10, transfers as in Figure 2), gated on CD4⁺Edited⁺FoxP3⁺ cells.

(B) Compilation of Helios⁺ or RORγ⁺ frequencies (as a proportion of pTreg cells) in spleen, colonic mLN and colon, grouped according to TCR specificity (from the same experiments as Figures 2C–2F, S2E, and S2F).

(C) Aggregated data (% Helios⁺ vs. RORγ⁺ among pTreg cells), color-coded according to antigen specificity.

(D) As (C), color-coded for the TCR cell of origin.

(E) Proportions of RORγ⁺, Helios⁺, and RORγ⁻Helios⁻ (DN) cells among TF2.2 pTreg cells in SPF, gnotobiotic mice monocolonized with *E. coli* Nissle or *C. ramosum*, or germfree hosts.

(F) The *Il6ra* locus in CD4⁺ T cells (congenically tagged with Thy1.1 or Thy1.1/2) was targeted by electroporation of Cas9/gRNA complexes[45] (or irrelevant gRNA as control), followed by standard TCR editing procedure before transfer into CD45.1/B6 hosts for 10 days. RORγ⁺ percent among pTreg cells were quantified in control or IL-6-receptor deleted cells. *$p < 0.05$, **$p < 0.01$, ***$p < 0.001$ by paired Student's *t* test. Each symbol or bar in (B), (E), and (F) represents an individual mouse. Each symbol in (C) and (D) represents one tissue in an individual mouse. Experiments from at least two independent experiments were pooled together. Only samples with more than 5 pTreg cells per TCR-edited population were included for analysis.

also edited with control or *Il6ra*-inactivating gRNAs, into the same hosts. The results showed that inactivating the IL-6 receptor in Tconv cells did not affect pTreg cell differentiation overall but significantly reduced the fraction of RORγ⁺ pTreg cells (Figure 3F). Thus, IL-6 signaling plays a crucial role in promoting RORγ expression in food-specific pTreg cells.

Different antigen/TCR pairs induce transcriptionally unique pTreg cells

These results showed that different classes of gut antigens led to different pTreg cell generation, numerically and phenotypically. To understand more fully if these different classes also led to phenotypically distinct Treg cell populations, we performed single cell RNA-sequencing (scRNA-seq) on newly generated pTreg cells expressing TF2.2, TF2.7, and TF2.6 (food-reactive); TM3.5, TM2.3, and TM1.2 (microbe-reactive); or TS2.3 and TS2.1 (self-reactive) TCRs 10 days after transfer (sorted based on FoxP3-GFP expression from pooled mLNs). We also analyzed cells that did not convert to FoxP3-positivity, as they might inform on what was missing in cells that did not become pTreg cells and/or on transition intermediates (Figure 4). A Tconv TCR control (TM1.2), which went through the same culture and transfer steps but does not develop into pTreg cells, was used as negative control (as were non-edited cells in other experiments; Figure S5). As references for normal Treg and Tconv cells, we included CD25hi Treg cells from the host mice as well as GFP$^+$ and GFP$^-$ cells from an age-matched *FoxP3-gfp* mouse (multiplexed by on-chip-multiplexing and hashtagging into the same 10× Genomics run).

The overall distribution of all cells in this experiment is shown in the uniform manifold approximation and projection (UMAP) of Figure 4A (data from a similar experiment in Figure S5). Tconv (Cl.0 and Cl.5) and Treg (Cl.2-4) cells were distinguished by the usual markers (Figures 4A, 4B, S5A, and S5B) and reproducibly confirmed by the position of control cells (host cells, TM1.2 edited cells, and mLN cells from a standard FoxP3-GFP mouse). A substantial fraction of donor-derived cells also mapped to a group of cells which included both GFP$^+$ pTreg and GFP$^-$ Tconv cells (Cl.1, hereafter "transitional"; Figure 4D).

Donor-derived pTreg cells localized to very different regions of the UMAP depending on the TCR expressed. Biological replicates with TF2.7 (different editing and different hosts, Figure 4D, left) established that these differences were indeed linked to the TCR/Ag pair and not artefactual to host or batch variations. Wheat-reactive TF2.2 and TF2.7 pTreg cells mapped predominantly to an aTreg cell cluster characterized by highly expressed *Rorc*, *Ikzf2, Maf*, and *Il10* (Figures 4B and 4D). In contrast, pTreg cells expressing the soy-reactive TF2.6 and self-reactive TS2.3 and TS2.1 dominated in the transitional cluster. With the microbe-reactive TM3.5 and TM2.3, pTreg cells were much more dispersed in the Treg cell space, with cells in the aTreg, rTreg, and transitional segments, as well as some cells close to the naive Tconv cluster. Importantly, these differences (scattered pTreg cells with TM3.5, mostly transitional cells with TS2.3, and some mature aTreg cells with TF2.2) were also seen in the independent scRNA-seq data of Figure S5. These differences in pTreg cell programs also corresponded to variations in the expression of typical Treg marker genes like *Il2ra*, *Ctla4*, or *Tnfrsf4* (Figure S5E), and the RORγ$^+$ Treg signature[47] was enriched in TF2.2 pTreg cells compared with TS2.3 pTreg cells (Figure S5F; TableS3). Thus, pTreg cell differentiation leads to marked aTreg cell phenotype (consistent with recent activation by antigen), among which the TCR/antigen combinations lead to distinct outcomes.

Figures 4D and S5C also revealed that the donor-derived cells that did not turn on FoxP3 (sorted as FoxP3-GFP-negative) did not fall as expected in the Tconv space of the UMAP but instead very close to fully differentiated pTreg cell in the transitional cluster (with the exception of TM2.3 and TM3.5, which remained more like resting Tconv cells). *Nr4a1* expression levels were comparable between Treg and Tconv groups, indicating both populations have undergone TCR activation (Figure 4D). Indeed, a comparison of pooled unconverted Tconv vs. pTreg cells in the transitional cluster found very few differences (8 genes are upregulated in Tconv cells and 21 genes up in Treg cells), with the striking exception of *FoxP3*, *GFP*, and *Il2ra* in Treg cells, as well as *Tcf7* and *Id2* in Tconv cells (Figures 4E and 4F). A previous report[48] with gliadin-reactive TCRs indicated that exposure to food antigens causes cognate CD4$^+$ T cells to adopt characteristics associated with anergy (*Izumo1r* [encodes FR4] and *Nt5e* [encodes CD73]) or follicular helpers (*Bcl6*). The first two were strongly represented in the unconverted Tconv cells of the transitional cluster (Figure 4G), strengthening the notion that pTreg cell differentiation is related to cells annotated as anergic. It thus appears that Tconv cells that fail to convert are actually at transitional stage and encompass virtually all the changes leading to pTreg state, except that they fail to induce *FoxP3* and *Il2ra*, almost reaching but not going beyond this tipping point.

Do pTreg cells persist as a memory pool?

Once induced, how long do pTreg cells persist in the absence of the inducing antigen? In other words, does the pTreg cell pool contain a memory compartment or is it continuously renewed? The questions speak to the nature of Treg cell memory.[49–51] It might be advantageous to maintain memory Treg cells, rapidly recruited immunoregulation preventing an over-exuberant secondary response by memory Tconv cells.[52] Conversely, transient "memory-less" Treg cell activity would avoid a cumulative state of generalized over-suppression.[53] Our experimental system allowed tracing of the fate of food-specific pTreg cells with varying antigen exposure (Figure 5A). After transfer of Tconv cells expressing either of two food-reactive TCRs into mice fed normal chow to elicit pTreg cell differentiation, some of the animals were switched to AFD, and maintained for 6–10 weeks (we verified, 1 week after such a switch, that food antigen had cleared and was no longer able to elicit pTreg cells). With continued antigen presence, pTreg cells persisted in roughly the same numbers as at day 10 (green in Figure 5B). These pTreg cells dropped after the long period without antigen (red bars), which varied between tissues and with different TCRs but remained always detectable and more numerous than in hosts never exposed to antigen (white). Finally, a short re-exposure to chow returned pTreg cells to constant-exposure levels (blue symbols). Tconv cells expressing the same TCRs tended to fluctuate less than pTreg cells (Figure 5B, right). These experiments establish that food-reactive pTreg cells can persist for long periods in the absence of antigen, a defining element of memory formation (given the numbers of cells, we cannot assess re-activation kinetics).

In terms of phenotype (Figure 5C), TF2.2-driven pTreg cells kept their usual low/mid level of RORγ$^+$ proportions. On the other hand, TF2.5 pTreg cells, which achieve very high RORγ$^+$ proportions, lost this almost completely in the SI and SI-draining mLN, while the phenotype was maintained in the colon and colon-draining mLNs, which we propose reflects the influence

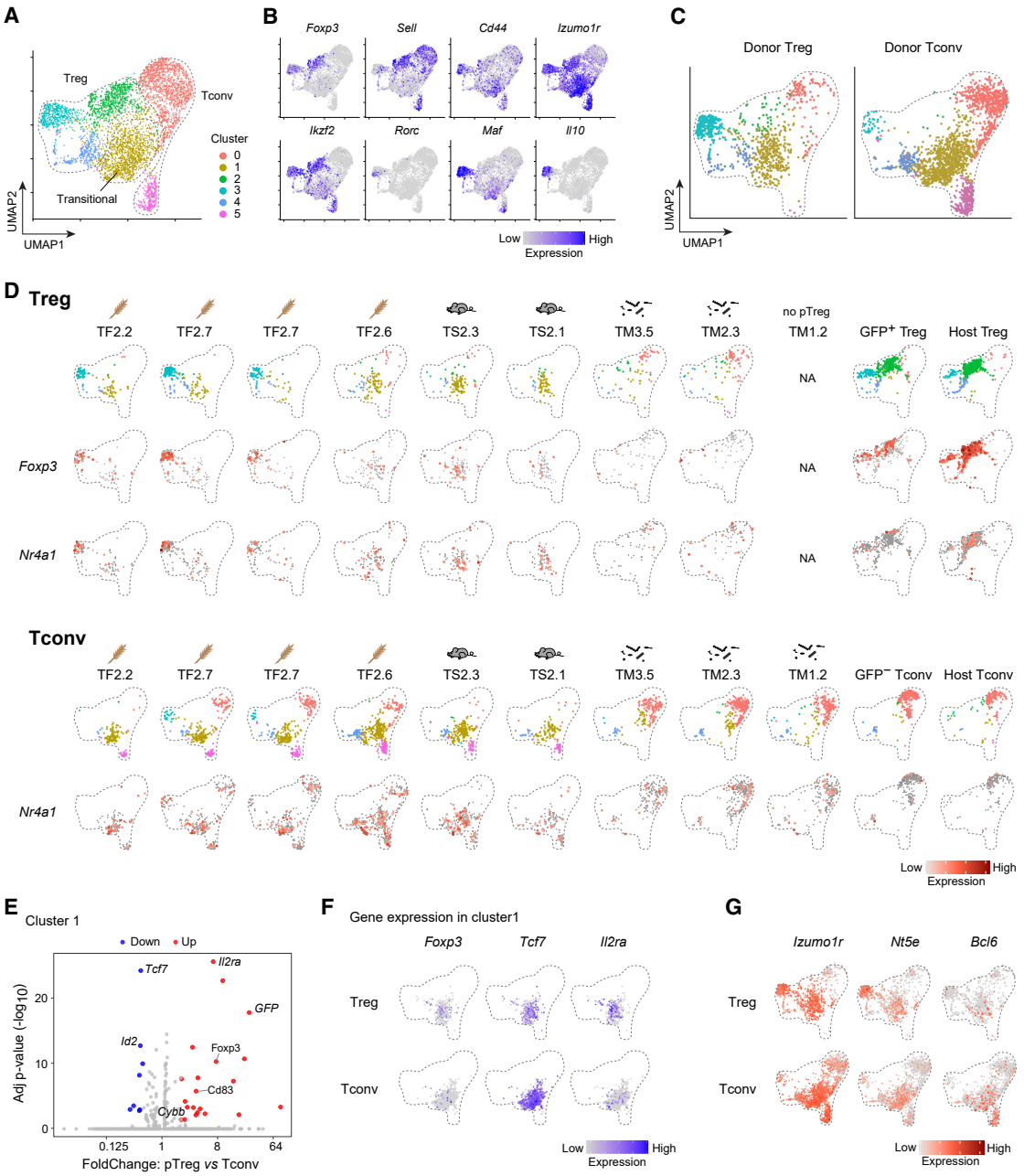

Figure 4. scRNA-seq reveals distinct transcriptomes in pTreg cells guided by different TCRs

Cells isolated from mLNs 10 days after adoptive transfer or from mLN of an age-matched FoxP3-GFP reporter mouse were analyzed by scRNA-seq analysis. Nine TCRs were used: TM3.5, TM2.3, and TM1.2 (*E. coli* Nissle reactive); TS2.3 and TS2.1 (self-reactive); and TF2.2, TF2.7, and TF2.6 (food reactive).

(A and B) (A) UMAP of scRNA-seq data encompassing all groups, annotation based on expression of key indicator genes (B) and on reference cells in (D).

(C) UMAP of pooled donor FoxP3^{+} pTreg and FoxP3^{-} Tconv cells.

(D) Position of cells from each group on the collective UMAP; FoxP3-GFP^{+} donor pTreg cells, Treg cells from a FoxP3-GFP reporter mouse, and CD25hi host Treg cells on the top; FoxP3-GFP^{-} Tconv cells, Tconv CD4^{+} cells from a FoxP3-GFP reporter mouse, and CD25neg host Tconv cells on the bottom. *FoxP3* and *Nr4a1* expression is highlighted for each sample.

(E) Volcano plot of differentially expressed genes between cluster 1 from pooled donor pTreg and Tconv cells. Red and blue dots represent genes significantly highly expressed in pTreg or Tconv cells, respectively. Statistical significance was determined using Wilcoxon rank-sum test. Highlighted genes meet FoldChange >2 with an adjusted p value < 0.05.

(F) UMAP feature plots showing genes expression of cluster 1 cells only, separated cells from donor pTreg (upper) or donor Tconv cells (lower).

(G) UMAP feature plots showing the expression of key T cell signatures in pooled donor Treg (top) and donor Tconv cells (bottom). Color intensity represents the log-normalized expression level for each gene. All plots of individual genes are scaled to the same color threshold to ensure comparability between groups (B, D, F, and G).

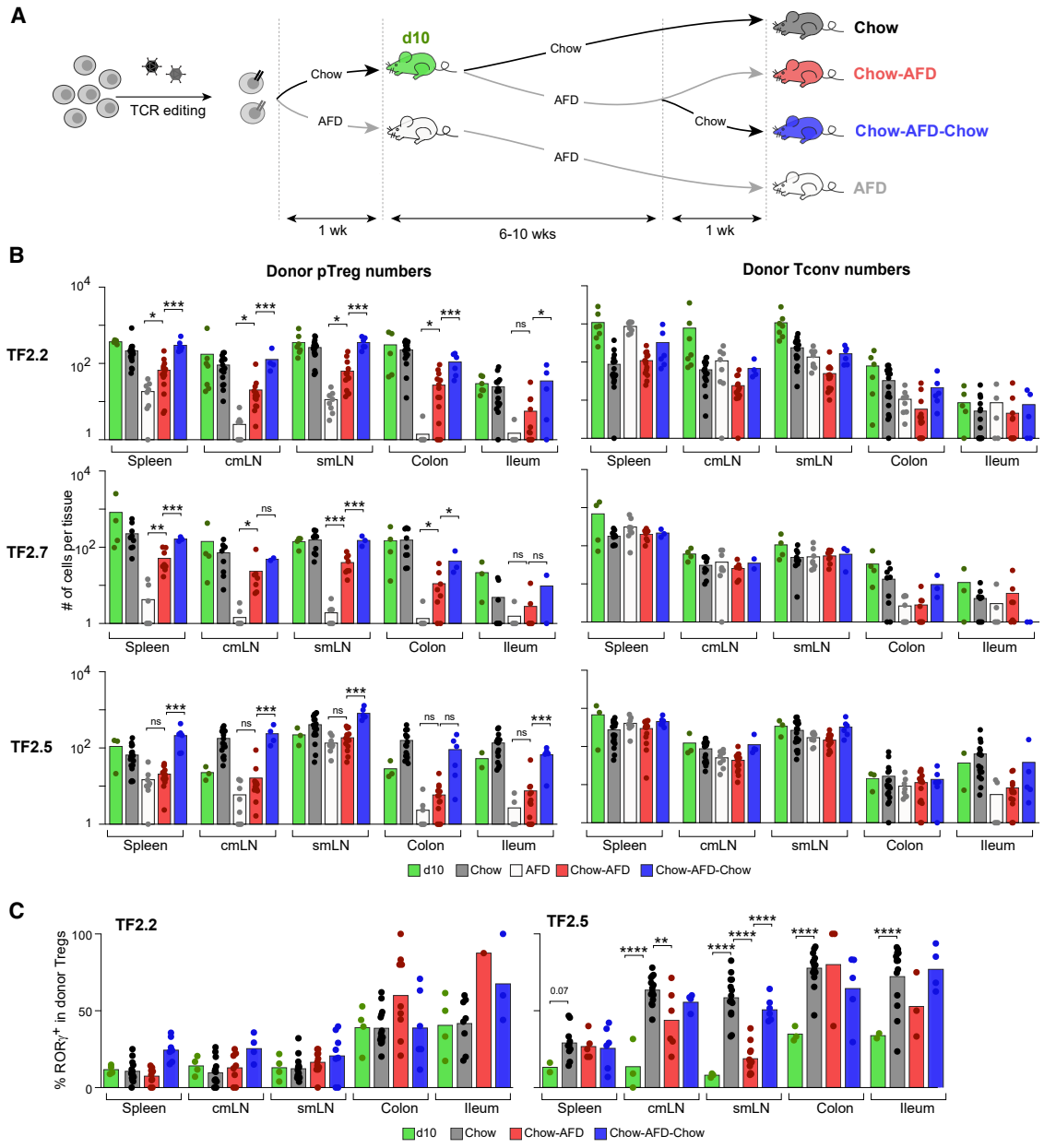

Figure 5. Memory in food-specific pTreg cells

(A) Experimental design. Tconv cells edited with food-reactive TCRs were transferred into a host fed normal chow for 1 week. Control hosts were maintained on an antigen-free diet (AFD) throughout the study. Subsequently, half of the antigen-exposed mice were switched to AFD for 6–10 weeks. To evaluate the effect of antigen re-exposure, a subset of these chow-AFD mice was switched back to normal chow for 1 week (chow-AFD-chow).

(B) Quantification of cell numbers of TF2.2, TF2.7, or TF2.5 TCR-expressing Tconv or pTreg cells in indicated tissues. Day 10 data (green bars) are from Figures 2D and 2F.

(C) Quantification of RORγ$^+$ Treg cell frequencies in the same experiments. Each dot represents an individual mouse; bars represent mean. $^*p < 0.05$, $^{**}p < 0.01$, and $^{***}p < 0.001$ (unpaired Student's *t* test). Mice from 2–4 independent experiments were pooled together.

of high microbial load. Thus, RORγ/Helios phenotypic changes can occur in pTreg cells independent of the initiating antigen.

Different antigen sources rely on different APCs

APCs, and in particular dendritic cells (DCs), exist in a spectrum types which differently influence the differentiation color of T cells to which they present antigens, including pTreg cell differentiation.[54,55] Recent studies using the ovalbumin (OVA) tolerance model have shown the importance of RORγ$^+$ APCs in regulating food-induced pTreg cells.[56–58] In contrast, other studies reported that conventional DCs play a dominant role in OVA-responsive pTreg cell differentiation.[59,60] To address this

contradiction and to broaden the analysis beyond OVA-driven responses, we leveraged our pTreg-inducing TCRs to analyze the involvement of different APCs in pTreg cell differentiation in response to bacterial, food, or self-antigens. In practice, we used as hosts two different lines of mice with selective antigen presentation defects. *Rorc*^{Cre} × *H2-Ab1*$^{fl/fl}$, hereafter *MHCII*$^{\Delta ROR\gamma}$, lack MHC class II molecules in RORγ$^+$ APCs, while *Clec9a*^{cre} × *H2-Ab1*$^{fl/fl}$ (*MHCII*$^{\Delta Clec9a}$) mice lack MHC class II expression in all type 1 conventional dendritic cells (cDC1s) and most cDC2s.[56,61]

We transferred Tconv cell edited as above to express bacteria, food, or self-reactive TCRs into these two mice (or cre-negative *H2-Ab1*$^{fl/fl}$ control littermate) (Figure 6A). In the representative experiment of Figure 6B, pTreg cell differentiation of TF2.2 expressing Tconv cells (food-reactive) was essentially abrogated in the *MHCII*$^{\Delta ROR\gamma}$ hosts but only marginally affected in the *MHCII*$^{\Delta Clec9a}$ hosts. Compiled data from several experiments (Figure 6C) revealed very different outcomes according to the TCR/antigen combination. pTreg cell differentiation from food-reactive T cells (TF2.2, TF3.3, and TF2.5) required MHC class II expression on RORγ$^+$ APCs, with little or no requirement for MHC class II on cDCs (for TF3.3, then affecting mostly RORγ$^-$ pTreg cells). The outcome was exactly opposite for the self-reactive TS2.3 and TS2.1 (no pTreg cells without cDC presentation, RORγ$^+$ APCs irrelevant). Microbe-reactive T cells (TM3.5) were partially affected by both deficiencies. The different baseline levels of pTreg cell induction in littermate control mice from two strains may reflect variations of antigen availability during digestion or affected by gut microbiota. Thus, the involvement of different APC subsets in gut pTreg cell differentiation varies with the type of TCR/antigen pairs.

The results were also interesting with regard to the phenotype of pTreg cells elicited in these partially defective hosts. For food-reactive T cells in *MHCII*$^{\Delta ROR\gamma}$ mice, both RORγ$^+$ and RORγ$^-$ pTreg cells were eliminated. The picture was more subtle for microbe-reactive TM3.5, the *MHCII*$^{\Delta ROR\gamma}$ deficiency preferentially affecting RORγ$^+$ pTreg cells and the *MHCII*$^{\Delta Clec9a}$ deficiency partially affecting both (and TS2.3 pTreg cells remained RORγ$^-$ in either context) (Figure 6C). These results indicate that it is not possible to make a 1-to-1 connection between the type of APC and the phenotype of pTreg cell whose differentiation it supports.

DISCUSSION

To explore how reactivity to different intestinal antigens controls T cell fate, more broadly than can be achieved with conventional transgenic mice, we performed a "mini-screen" by editing into CD4$^+$ T cells a panel of TCRs originating from different types of colonic T cells, with a range of antigen specificity. Transfer experiments with cells expressing these TCRs revealed a wide range in the ability to support pTreg cell differentiation and to yield RORγ$^+$ vs. Helios$^+$ pTreg cells, depending on the type of cell from which the TCRs originated and the type of antigen they recognize. These results demonstrate the primacy of the TCR in determining CD4$^+$ T cell fate at organismal barriers and have implications for tolerogenic cell therapy.

The present results bring two important pieces of information concerning pTreg cells. First, pTreg cells are not necessarily RORγ$^+$ and vice versa. We have previously argued[9] that this relationship is not as obligate as often depicted in the literature, but the present data should help close the debate: pTreg cells in our transfer experiments adopted a range of RORγ$^+$/Helios$^+$ phenotypes. Most biased were pTreg cells driven by self-antigens, which were uniformly RORγ$^-$, bacteria antigens promoted a majority of RORγ$^+$ Treg cells, while food antigens enabled both. Indeed, even for pTreg cells that express the same TCR, the proportion of RORγ$^+$ Treg cells was tissue dependent, being higher in the colon than in other tissues, and evolved over time. Second, pTreg cells are not only confined to the GALT but disseminate widely in systemic lymphoid organs like the spleen or scLNs. Indeed, in absolute numbers, the spleen is where most pTreg cells reside, and they persist there long after differentiation. This dispersion may reflect continuous circulation of the pTreg cells or trafficking outside of the GALT of APCs loaded with intestinal antigens. More generally, it ties in with the idea that T cell activation in the intestine can have unexpected consequences far outside the gut.[47,62–65]

In addition, the profiling data provide an intriguing perspective on the transcriptional changes that occur in newly generated pTreg cells in an otherwise unperturbed host. These generally matched previous reports[13] but also brought out interesting divergences in pTreg cells driven by different TCRs/antigen combinations. The most arresting observation might concern those cells that expressed the same tolerogenic TCR but did not become FoxP3-positive, as evidenced by both reporter expression and RNA-seq. We speculate that these represent an intermediate state reaching but not going through the tipping point of acquiring FoxP3. These cells might be related to the "wannabe" Treg-like cells that exist in FoxP3-deficient mice or humans and also have many Treg cell characteristics.[66–68] In this respect, pTreg cell differentiation might then behave much like thymic tTreg cell differentiation, with its late acquisition of *FoxP3* and *Il2ra* expression in intermediates that differentiate independently of FoxP3.[69]

The breadth of the TCRs studied here revealed striking differences between individual TCRs in directing local T cell fate. This observation differed from the notion that activation of any T cell by its cognate antigen in the gut could lead to pTreg cell differentiation, driven by unique conditions (high TGFβ, retinoic acid, etc.) and APCs found there. TCRs originally isolated from Treg cells promoted pTreg cell development (although to variable extents), while Tconv-restricted TCRs largely failed to do so, cells maintaining a Tconv phenotype (with high proliferation in one case). Furthermore, TCRs derived from RORγ$^+$ Treg cells preferentially guided the differentiation of RORγ$^+$ pTreg cells. There is a degree of circular reasoning in this notion that individual TCRs drive T cell differentiation back to their cell of origin, but it indicates that TCRs carry an intrinsic potential toward specific cell fates. A recent study of CD8$^+$ T cells similarly showed that distinct clonotypes exhibit biased differentiation toward memory precursors or terminal effector cells, regardless of shared inflammatory cues or stochastic influences.[70] This influence likely reflects the TCR determining the antigen, the type of APCs that present the antigens, and the context in which activation occurs, as well as strength and kinetics of downstream signaling upon antigen recognition. However, the final outcome is also influenced by environmental cues. IL-6, previously found to modulate

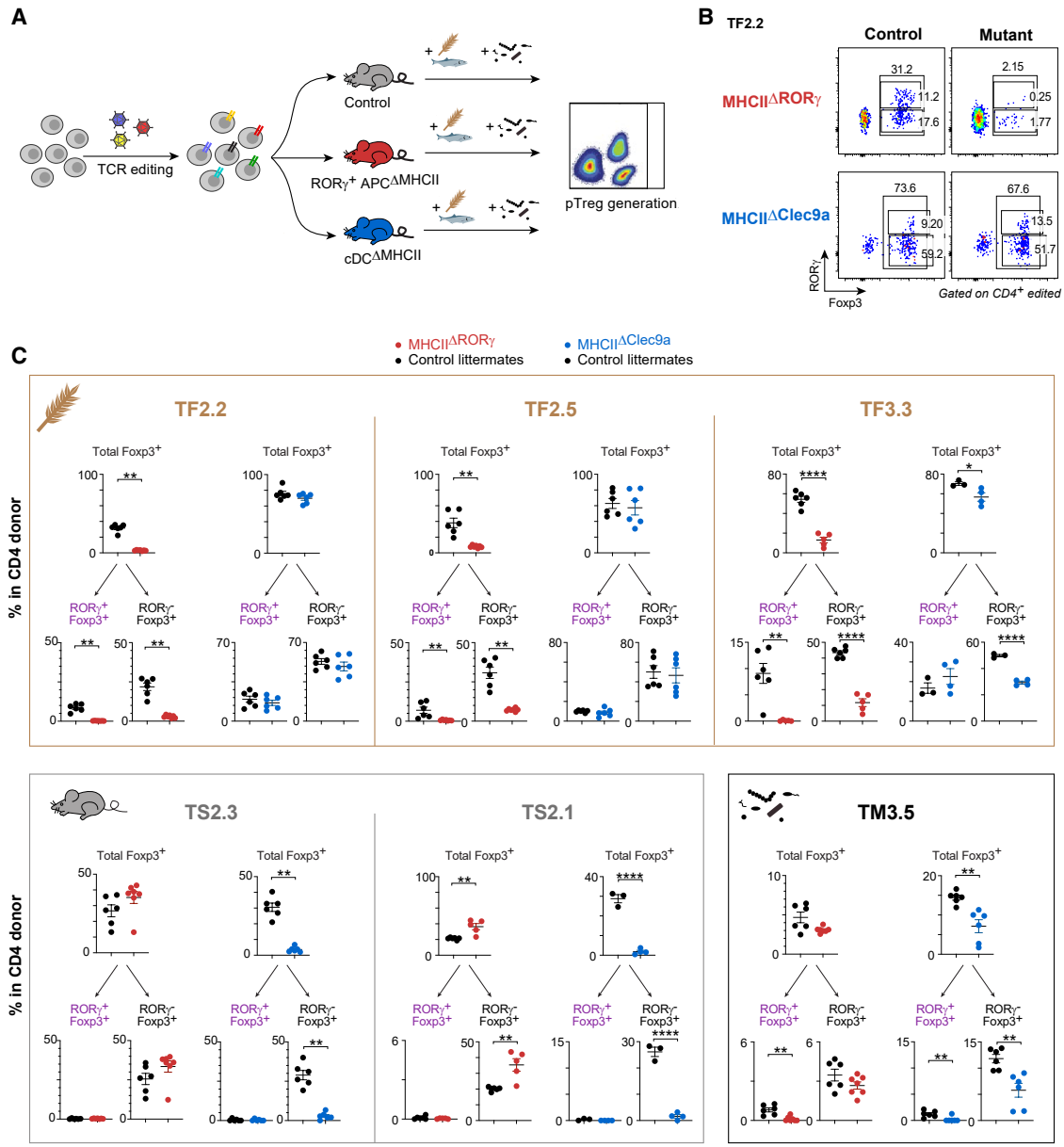

Figure 6. RORγ⁺ APCs or cDCs support pTreg cells driven by different TCR/antigen pairs

(A) Experimental design. TCR-edited Tconv cells specific for food, microbe, or self-antigens were transferred into hosts lacking MHC class II on RORγ⁺ APCs (red) or on cDCs (blue) or control littermates, and pTreg cell differentiation was assessed 10 days later.

(B) Representative plots showing pTreg cell generation for TF2.2-edited cells in the indicated mutant host and matched littermate controls (gated on CD4⁺E-dited⁺ cells).

(C) Compiled quantification of mLN pTreg cells generated from four groups of TCR-edited Tconv cells, shown as whole FoxP3⁺ cells (as a proportion of donor cells, top), or split into RORγ⁺FoxP3⁺ and RORγ⁺FoxP3⁺ subsets. Each dot represents an individual mouse; bars denote mean ± SEM. Statistical significance determined by unpaired Student's *t* test, $*p < 0.05$, $**p < 0.01$, and $****p < 0.0001$. Results are combined from one to three independent experiments.

the proportion of RORγ⁺ Treg cells,[6,15,46] was required here for effective generation of RORγ⁺ pTreg cells.

Self-reactive TCRs generally lead to Treg cell differentiation by clonal deviation in the thymus. The self-reactive TCRs used here stemmed originally from RORγ⁻ Treg cells in the gut, and we do not know if those cells were thymically differentiated tTreg cells or pTreg cells differentiated in the GALT. In a sense, editing these TCRs into Tconv cells reverted the normal Treg cell differentiation process, and the results establish that pTreg cell generation can represent a safety net for reactivity toward self-antigens that failed to be tolerized in the thymus. In future experiments, it will be interesting to see whether these would actually escape thymic tolerance or would instead result in early tTreg cell differentiation.

The APCs that drive the differentiation of pTreg cells and their subsets is an area of keen interest.[31,56,58,59,71,72] Our study

highlighted the notion that different APCs are required for the generation of pTreg cells in response to different sources of antigen. At one end of the spectrum, differentiation of TS2.3 and TS2.1 pTreg cells driven by self-antigen was wholly dependent on cDCs, with no requirement for RORγ⁺ APCs. Diametrically opposite, the impairment of RORγ⁺ APCs disrupted the generation of food-antigen-specific pTreg cells, affecting both RORγ⁺ and RORγ⁻ Treg subsets, with a minor impact of cDCs, variable with TCRs. This connection is consistent with and broadens several reports in the OT-II/oral-OVA model.[56,58,71,72] Finally, pTreg cells induced with the TM3.5 TCR in response to *E. coli* antigen were intermediate, with a partial dependence on both cDCs and RORγ⁺ APCs. Previous studies had also shown a dominance of RORγ⁺ APCs in pTreg cell differentiation in the HH7-2/*Helicobacter* system.[31] Our data suggest that, depending on the nature of the microbe, presentation of microbial antigens relies on different APC subsets to induce pTreg cells, in line with the earlier observation in *Listeria* vs. *SFB* comparisons, where T cell effector functions were determined by the type of bacteria that produced the antigen rather than by the antigen itself.[73]

In conclusion, the notion that a TCR drives the differentiation of uncommitted T cells toward the phenotype of the cell in which it was originally discovered has implication for T cell identity. It is not simply stochastically determined by encounters with cytokines, costimulatory molecules, or other non-specific influences, but it is to some extent pre-determined by the TCR itself. This notion has direct implications for T cell engineering: it does not suffice to equip a naive T cell with a receptor whose specificity will drive it to a given location, but the use of a Treg cell-derived TCR will facilitate finding the proper antigen and APC to achieve the desired tolerogenic state.

Limitations of the study

Although we know the source of the antigens, we do not know the exact protein involved. Hence, the quantity of antigenic peptide available for presentation to the different TCRs is unknown, and this may contribute to differences in pTreg cell induction or APC requirements. We will never know whether our TCRs initially originated from tTreg cells or pTreg cells, and whether they would be normally selected into the conventional T cell pool. The experiments demonstrate the capacity of these TCRs to drive pTreg cell differentiation if expressed in Tconv cells, but they do not reveal whether the corresponding endogenous clones normally develop as pTreg cells or tTreg cells (although we suspect some of each).

RESOURCE AVAILABILITY

Lead contact

Requests for further information, resources, and reagents should be directed to and will be fulfilled by the lead contact, Prof. Christophe Benoist (cbdm@hms.harvard.edu).

Materials availability

AAV vectors used in this study have been deposited at Addgene or are available from the authors upon qualified request.

Data and code availability

The scRNA-seq data reported in this paper have been deposited in the Gene Expression Omnibus (GEO) database under accession GEO: GSE301231. No specific code was developed for this work, which only used generally available software.

ACKNOWLEDGMENTS

We thank Drs. S. Ramanan and M. Sassone-Corsi who discovered the TCRs used here; Drs. D. Kasper, E. Martens, and D. Littman for provision of bacterial strains; K. Hattori, C. Araneo, M. Henderson, V. Piekarsa, and I. Magill for help with mice, cell sorting, and single-cell profiling; and Dr. J. Chouinard and J. Espinal (LabDiet) for samples of diet components. This work was funded by NIH grants AI182126 and AI150686 to C.B. and D.M.; funding from the Pew Trust, Parker Institute for Cancer Immunotherapy, CRISPR Cures for Cancer, and Grand Multiple Myeloma Translational Initiative to J.E.; and an NIAID DP2 award (DP2AI171116) and a Pew Biomedical Scholar Award to C.C.B. V.C. was supported by a St. Baldrick's Fellowship, W.A.N. was supported by the Swedish Society for Medical Research and the Swedish Research Council, C.H.W. was supported by the NSF Graduate Research Fellowship Program at UCSF, X.C. was supported by Gene Lay Institute Postdoctoral Fellowship, and D.L.O. was supported by a NIDDK T32 Postdoctoral Training Grant (T32DK007477) and a CRI Irvington Postdoctoral Fellowship (CRI4983).

AUTHOR CONTRIBUTIONS

X.C., C.H.W., Y.F.P., A.G., Y.C., V.C., Y.C., and J.A. performed the experiments; W.A.N. and D.L.O. provided materials and discussed interpretations; X.C., C.H.W., W.A.N., Y.C., V.C., C.C.B., J.E., D.M., and C.B. designed the study as well as analyzed and interpreted the data; X.C. and C.B. wrote the first draft; and all authors edited the manuscript.

DECLARATION OF INTERESTS

The authors declare no competing interests.

STAR★METHODS

Detailed methods are provided in the online version of this paper and include the following:

- KEY RESOURCES TABLE
- METHOD DETAILS
  - Mice
  - TCRs
  - TCR editing of primary CD4⁺ T cells
  - *In vitro* screening of antigen reactivity
  - Gene inactivation by electroporation of Cas9/gRNA complexes
  - Bacteria culture and colonization
  - Cell transfers and donor cell assessment
  - Lymphocyte isolation from tissues
  - Flow cytometry
  - scRNA-seq pTreg profiling
- QUANTIFICATION AND STATISTICAL ANALYSIS

SUPPLEMENTAL INFORMATION

Supplemental information can be found online at https://doi.org/10.1016/j.immuni.2026.07.001.

Received: August 22, 2025
Revised: March 18, 2026
Accepted: July 5, 2026
Published: July 28, 2026

REFERENCES

1. Ansaldo, E., Farley, T.K., and Belkaid, Y. (2021). Control of Immunity by the Microbiota. Annu. Rev. Immunol. *39*, 449–479. https://doi.org/10.1146/annurev-immunol-093019-112348.

2. Benamar, M., Chen, Q., Martinez-Blanco, M., and Chatila, T.A. (2023). Regulatory T cells in allergic inflammation. Semin. Immunol. *70*, 101847. https://doi.org/10.1016/j.smim.2023.101847.

3. Ivanov, I.I., Atarashi, K., Manel, N., Brodie, E.L., Shima, T., Karaoz, U., Wei, D., Goldfarb, K.C., Santee, C.A., Lynch, S.V., et al. (2009). Induction of intestinal Th17 cells by segmented filamentous bacteria. Cell *139*, 485–498. https://doi.org/10.1016/j.cell.2009.09.033.

4. Ansaldo, E., Slayden, L.C., Ching, K.L., Koch, M.A., Wolf, N.K., Plichta, D.R., Brown, E.M., Graham, D.B., Xavier, R.J., Moon, J.J., et al. (2019). Akkermansia muciniphila induces intestinal adaptive immune responses during homeostasis. Science *364*, 1179–1184. https://doi.org/10.1126/science.aaw7479.

5. Lathrop, S.K., Bloom, S.M., Rao, S.M., Nutsch, K., Lio, C.W., Santacruz, N., Peterson, D.A., Stappenbeck, T.S., and Hsieh, C.S. (2011). Peripheral education of the immune system by colonic commensal microbiota. Nature *478*, 250–254. https://doi.org/10.1038/nature10434.

6. Sefik, E., Geva-Zatorsky, N., Oh, S., Konnikova, L., Zemmour, D., McGuire, A.M., Burzyn, D., Ortiz-Lopez, A., Lobera, M., Yang, J., et al. (2015). Individual intestinal symbionts induce a distinct population of RORγ^{+} regulatory T cells. Science *349*, 993–997. https://doi.org/10.1126/science.aaa9420.

7. Bilate, A.M., Bousbaine, D., Mesin, L., Agudelo, M., Leube, J., Kratzert, A., Dougan, S.K., Victora, G.D., and Ploegh, H.L. (2016). Tissue-specific emergence of regulatory and intraepithelial T cells from a clonal T cell precursor. Sci. Immunol. *1*, eaaf7471. https://doi.org/10.1126/sciimmunol.aaf7471.

8. Wegorzewska, M.M., Glowacki, R.W.P., Hsieh, S.A., Donermeyer, D.L., Hickey, C.A., Horvath, S.C., Martens, E.C., Stappenbeck, T.S., and Allen, P.M. (2019). Diet modulates colonic T cell responses by regulating the expression of a *Bacteroides thetaiotaomicron* antigen. Sci. Immunol. *4*, eaau9079. https://doi.org/10.1126/sciimmunol.aau9079.

9. Ramanan, D., Pratama, A., Zhu, Y., Venezia, O., Sassone-Corsi, M., Chowdhary, K., Galván-Peña, S., Sefik, E., Brown, C., Gélineau, A., et al. (2023). Regulatory T cells in the face of the intestinal microbiota. Nat. Rev. Immunol. *23*, 749–762. https://doi.org/10.1038/s41577-023-00890-w.

10. Hoeppli, R.E., MacDonald, K.G., Levings, M.K., and Cook, L. (2016). How antigen specificity directs regulatory T-cell function: self, foreign and engineered specificity. HLA *88*, 3–13. https://doi.org/10.1111/tan.12822.

11. Curotto de Lafaille, M.A., Kutchukhidze, N., Shen, S., Ding, Y., Yee, H., and Lafaille, J.J. (2008). Adaptive Foxp3+ regulatory T cell-dependent and -independent control of allergic inflammation. Immunity *29*, 114–126. https://doi.org/10.1016/j.immuni.2008.05.010.

12. Haribhai, D., Williams, J.B., Jia, S., Nickerson, D., Schmitt, E.G., Edwards, B., Ziegelbauer, J., Yassai, M., Li, S.H., Relland, L.M., et al. (2011). A requisite role for induced regulatory T cells in tolerance based on expanding antigen receptor diversity. Immunity *35*, 109–122. https://doi.org/10.1016/j.immuni.2011.03.029.

13. van der Veeken, J., Campbell, C., Pritykin, Y., Schizas, M., Verter, J., Hu, W., Wang, Z.M., Matheis, F., Mucida, D., Charbonnier, L.M., et al. (2022). Genetic tracing reveals transcription factor Foxp3-dependent and Foxp3-independent functionality of peripherally induced Treg cells. Immunity *55*, 1173–1184.e7. https://doi.org/10.1016/j.immuni.2022.05.010.

14. Yilmazer, A., Zevla, D.M., Malmkvist, R., Rodríguez, C.A.B., Undurraga, P., Kirgin, E., Boernert, M., Voehringer, D., Kershaw, O., Schlenner, S., et al. (2023). Selective ablation of thymic and peripheral Foxp3+ regulatory T cell development. Front. Immunol. *14*, 1298938. https://doi.org/10.3389/fimmu.2023.1298938.

15. Ohnmacht, C., Park, J.H., Cording, S., Wing, J.B., Atarashi, K., Obata, Y., Gaboriau-Routhiau, V., Marques, R., Dulauroy, S., Fedoseeva, M., et al. (2015). The microbiota regulates type 2 immunity through RORγ^{+} T cells. Science *349*, 989–993. https://doi.org/10.1126/science.aac4263.

16. Neumann, C., Blume, J., Roy, U., Teh, P.P., Vasanthakumar, A., Beller, A., Liao, Y., Heinrich, F., Arenzana, T.L., Hackney, J.A., et al. (2019). c-Maf-dependent Treg cell control of intestinal TH17 cells and IgA establishes host-microbiota homeostasis. Nat. Immunol. *20*, 471–481. https://doi.org/10.1038/s41590-019-0316-2.

17. Xu, M., Pokrovskii, M., Ding, Y., Yi, R., Au, C., Harrison, O.J., Galan, C., Belkaid, Y., Bonneau, R., and Littman, D.R. (2018). c-MAF-dependent regulatory T cells mediate immunological tolerance to a gut pathobiont. Nature *554*, 373–377. https://doi.org/10.1038/nature25500.

18. Britton, G.J., Contijoch, E.J., Mogno, I., Vennaro, O.H., Llewellyn, S.R., Ng, R., Li, Z., Mortha, A., Merad, M., Das, A., et al. (2019). Microbiotas from humans with inflammatory bowel disease alter the balance of gut Th17 and RORγt^{+} regulatory T cells and exacerbate colitis in mice. Immunity *50*, 212–224.e4. https://doi.org/10.1016/j.immuni.2018.12.015.

19. Bhattacharjee, A., Burr, A.H.P., Overacre-Delgoffe, A.E., Tometich, J.T., Yang, D., Huckestein, B.R., Linehan, J.L., Spencer, S.P., Hall, J.A., Harrison, O.J., et al. (2021). Environmental enteric dysfunction induces regulatory T cells that inhibit local CD4^{+} T cell responses and impair oral vaccine efficacy. Immunity *54*, 1745–1757.e7. https://doi.org/10.1016/j.immuni.2021.07.005.

20. Abdel-Gadir, A., Stephen-Victor, E., Gerber, G.K., Noval Rivas, M., Wang, S., Harb, H., Wang, L., Li, N., Crestani, E., Spielman, S., et al. (2019). Microbiota therapy acts via a regulatory T cell MyD88/RORγt pathway to suppress food allergy. Nat. Med. *25*, 1164–1174. https://doi.org/10.1038/s41591-019-0461-z.

21. Chowdhary, K., Léon, J., Mathis, D., and Benoist, C. (2024). An integrated transcription factor framework for Treg identity and diversity. Proc. Natl. Acad. Sci. USA *121*, e2411301121. https://doi.org/10.1073/pnas.2411301121.

22. Wohlfert, E.A., Grainger, J.R., Bouladoux, N., Konkel, J.E., Oldenhove, G., Ribeiro, C.H., Hall, J.A., Yagi, R., Naik, S., Bhairavabhotla, R., et al. (2011). GATA3 controls Foxp3(+) regulatory T cell fate during inflammation in mice. J. Clin. Investig. *121*, 4503–4515. https://doi.org/10.1172/JCI57456.

23. Wang, Y., Su, M.A., and Wan, Y.Y. (2011). An essential role of the transcription factor GATA-3 for the function of regulatory T cells. Immunity *35*, 337–348. https://doi.org/10.1016/j.immuni.2011.08.012.

24. Schiering, C., Krausgruber, T., Chomka, A., Fröhlich, A., Adelmann, K., Wohlfert, E.A., Pott, J., Griseri, T., Bollrath, J., Hegazy, A.N., et al. (2014). The alarmin IL-33 promotes regulatory T-cell function in the intestine. Nature *513*, 564–568. https://doi.org/10.1038/nature13577.

25. Burzyn, D., Kuswanto, W., Kolodin, D., Shadrach, J.L., Cerletti, M., Jang, Y., Sefik, E., Tan, T.G., Wagers, A.J., Benoist, C., et al. (2013). A special population of regulatory T cells potentiates muscle repair. Cell *155*, 1282–1295. https://doi.org/10.1016/j.cell.2013.10.054.

26. Kim, K.S., Hong, S.W., Han, D., Yi, J., Jung, J., Yang, B.G., Lee, J.Y., Lee, M., and Surh, C.D. (2016). Dietary antigens limit mucosal immunity by inducing regulatory T cells in the small intestine. Science *351*, 858–863. https://doi.org/10.1126/science.aac5560.

27. Thornton, A.M., Korty, P.E., Tran, D.Q., Wohlfert, E.A., Murray, P.E., Belkaid, Y., and Shevach, E.M. (2010). Expression of Helios, an Ikaros transcription factor family member, differentiates thymic-derived from peripherally induced Foxp3+ T regulatory cells. J. Immunol. *184*, 3433–3441. https://doi.org/10.4049/jimmunol.0904028.

28. Pratama, A., Schnell, A., Mathis, D., and Benoist, C. (2020). Developmental and cellular age direct conversion of CD4^{+} T cells into RORγ^{+} or Helios^{+} colon Treg cells. J. Exp. Med. *217*, e20190428. https://doi.org/10.1084/jem.20190428.

29. Ramanan, D., Chowdhary, K., Candéias, S.M., Sassone-Corsi, M., Gelineau, A., Mathis, D., and Benoist, C. (2023). Homeostatic, repertoire and transcriptional relationships between colon T regulatory cell subsets. Proc. Natl. Acad. Sci. USA *120*, e2311566120. https://doi.org/10.1073/pnas.2311566120.

30. Lyu, M., Suzuki, H., Kang, L., Gaspal, F., Zhou, W., Goc, J., Zhou, L., Zhou, J., Zhang, W., et al.; JRI Live Cell Bank (2022). ILC3s select microbiota-specific regulatory T cells to establish tolerance in the gut. Nature *610*, 744–751. https://doi.org/10.1038/s41586-022-05141-x.

31. Kedmi, R., Najar, T.A., Mesa, K.R., Grayson, A., Kroehling, L., Hao, Y., Hao, S., Pokrovskii, M., Xu, M., Talbot, J., et al. (2022). A RORγ^{+} cell

instructs gut microbiota-specific Treg cell differentiation. Nature *610*, 737–743. https://doi.org/10.1038/s41586-022-05089-y.

32. Wang, J., Lareau, C.A., Bautista, J.L., Gupta, A.R., Sandor, K., Germino, J., Yin, Y., Arvedson, M.P., Reeder, G.C., Cramer, N.T., et al. (2021). Single-cell multiomics defines tolerogenic extrathymic Aire-expressing populations with unique homology to thymic epithelium. Sci. Immunol. *6*, eabl5053. https://doi.org/10.1126/sciimmunol.abl5053.

33. Yissachar, N., Zhou, Y., Ung, L., Lai, N.Y., Mohan, J.F., Ehrlicher, A., Weitz, D.A., Kasper, D.L., Chiu, I.M., Mathis, D., et al. (2017). An intestinal organ culture system uncovers a role for the nervous system in microbe-immune crosstalk. Cell *168*, 1135–1148.e12. https://doi.org/10.1016/j.cell.2017.02.009.

34. Zhu, Y., Meerschaert, K.A., Galvan-Pena, S., Bin, N.R., Yang, D., Basu, H., Kawamoto, R., Shalaby, A., Liberles, S.D., Mathis, D., et al. (2024). A chemogenetic screen reveals that Trpv1-expressing neurons control regulatory T cells in the gut. Science *385*, eadk1679. https://doi.org/10.1126/science.adk1679.

35. Solomon, B.D., and Hsieh, C.S. (2016). Antigen-Specific Development of Mucosal Foxp3^{+}RORγ^{+} T Cells from Regulatory T Cell Precursors. J. Immunol. *197*, 3512–3519. https://doi.org/10.4049/jimmunol.1601217.

36. Nyberg, W.A., Ark, J., To, A., Clouden, S., Reeder, G., Muldoon, J.J., Chung, J.Y., Xie, W.H., Allain, V., Steinhart, Z., et al. (2023). An evolved AAV variant enables efficient genetic engineering of murine T cells. Cell *186*, 446–460.e19. https://doi.org/10.1016/j.cell.2022.12.022.

37. Nagashima, K., Zhao, A., Atabakhsh, K., Bae, M., Blum, J.E., Weakley, A., Jain, S., Meng, X., Cheng, A.G., Wang, M., et al. (2023). Mapping the T cell repertoire to a complex gut bacterial community. Nature *621*, 162–170. https://doi.org/10.1038/s41586-023-06431-8.

38. Moran, A.E., Holzapfel, K.L., Xing, Y., Cunningham, N.R., Maltzman, J.S., Punt, J., and Hogquist, K.A. (2011). T cell receptor signal strength in Treg and iNKT cell development demonstrated by a novel fluorescent reporter mouse. J. Exp. Med. *208*, 1279–1289. https://doi.org/10.1084/jem.20110308.

39. Zemmour, D., Zilionis, R., Kiner, E., Klein, A.M., Mathis, D., and Benoist, C. (2018). Single-cell gene expression reveals a landscape of regulatory T cell phenotypes shaped by the TCR. Nat. Immunol. *19*, 291–301. https://doi.org/10.1038/s41590-018-0051-0.

40. Blum, J.E., Kong, R., Schulman, E.A., Chen, F.M., Upadhyay, R., Romero-Meza, G., Littman, D.R., Fischbach, M.A., Nagashima, K., and Sattely, E.S. (2026). Identification and characterization of dietary antigens in oral tolerance. Sci. Immunol. *11*, eaeb4684. https://doi.org/10.1126/sciimmunol.aeb4684.

41. Faith, J.J., Ahern, P.P., Ridaura, V.K., Cheng, J., and Gordon, J.I. (2014). Identifying gut microbe-host phenotype relationships using combinatorial communities in gnotobiotic mice. Sci. Transl. Med. *6*, 220ra11. https://doi.org/10.1126/scitranslmed.3008051.

42. Geva-Zatorsky, N., Sefik, E., Kua, L., Pasman, L., Tan, T.G., Ortiz-Lopez, A., Yanortsang, T.B., Yang, L., Jupp, R., Mathis, D., et al. (2017). Mining the human gut microbiota for immunomodulatory organisms. Cell *168*, 928–943.e11. https://doi.org/10.1016/j.cell.2017.01.022.

43. Liu, Y., Fatheree, N.Y., Dingle, B.M., Tran, D.Q., and Rhoads, J.M. (2013). Lactobacillus reuteri DSM 17938 changes the frequency of Foxp3^{+} regulatory T cells in the intestine and mesenteric lymph node in experimental necrotizing enterocolitis. PLoS One *8*, e56547. https://doi.org/10.1371/journal.pone.0056547.

44. Kuczma, M.P., Szurek, E.A., Cebula, A., Chassaing, B., Jung, Y.J., Kang, S.M., Fox, J.G., Stecher, B., and Ignatowicz, L. (2020). Commensal epitopes drive differentiation of colonic T_{regs}. Sci. Adv. *6*, eaaz3186. https://doi.org/10.1126/sciadv.aaz3186.

45. Hultquist, J.F., Hiatt, J., Schumann, K., McGregor, M.J., Roth, T.L., Haas, P., Doudna, J.A., Marson, A., and Krogan, N.J. (2019). CRISPR-Cas9 genome engineering of primary CD4(+) T cells for the interrogation of HIV-host factor interactions. Nat. Protoc. *14*, 1–27. https://doi.org/10.1038/s41596-018-0069-7.

46. Yan, Y., Ramanan, D., Rozenberg, M., McGovern, K., Rastelli, D., Vijaykumar, B., Yaghi, O., Voisin, T., Mosaheb, M., Chiu, I., et al. (2021). Interleukin-6 produced by enteric neurons regulates the number and phenotype of microbe-responsive regulatory T cells in the gut. Immunity *54*, 499–513.e5. https://doi.org/10.1016/j.immuni.2021.02.002.

47. Hanna, B.S., Wang, G., Galván-Peña, S., Mann, A.O., Ramirez, R.N., Muñoz-Rojas, A.R., Smith, K., Wan, M., Benoist, C., and Mathis, D. (2023). The gut microbiota promotes distal tissue regeneration via RORγ^{+} regulatory T cell emissaries. Immunity *56*, 829–846.e8. https://doi.org/10.1016/j.immuni.2023.01.033.

48. Hong, S.-W., Krueger, P.D., Osum, K.C., Dileepan, T., Herman, A., Mueller, D.L., and Jenkins, M.K. (2022). Immune tolerance of food is mediated by layers of CD4+ T cell dysfunction. Nature *607*, 762–768. https://doi.org/10.1038/s41586-022-04916-6.

49. Rosenblum, M.D., Gratz, I.K., Paw, J.S., Lee, K., Marshak-Rothstein, A., and Abbas, A.K. (2011). Response to self antigen imprints regulatory memory in tissues. Nature *480*, 538–542. https://doi.org/10.1038/nature10664.

50. Sanchez, A.M., Zhu, J., Huang, X., and Yang, Y. (2012). The development and function of memory regulatory T cells after acute viral infections. J. Immunol. *189*, 2805–2814. https://doi.org/10.4049/jimmunol.1200645.

51. Rowe, J.H., Ertelt, J.M., Xin, L., and Way, S.S. (2012). Pregnancy imprints regulatory memory that sustains anergy to fetal antigen. Nature *490*, 102–106. https://doi.org/10.1038/nature11462.

52. Rosenblum, M.D., Way, S.S., and Abbas, A.K. (2016). Regulatory T cell memory. Nat. Rev. Immunol. *16*, 90–101. https://doi.org/10.1038/nri.2015.1.

53. van der Veeken, J., Gonzalez, A.J., Cho, H., Arvey, A., Hemmers, S., Leslie, C.S., and Rudensky, A.Y. (2016). Memory of inflammation in regulatory T cells. Cell *166*, 977–990. https://doi.org/10.1016/j.cell.2016.07.006.

54. Eisenbarth, S.C. (2019). Dendritic cell subsets in T cell programming: location dictates function. Nat. Rev. Immunol. *19*, 89–103. https://doi.org/10.1038/s41577-018-0088-1.

55. Kedmi, R., and Littman, D.R. (2024). Antigen-presenting cells as specialized drivers of intestinal T cell functions. Immunity *57*, 2269–2279. https://doi.org/10.1016/j.immuni.2024.09.011.

56. Cabric, V., Franco, P.Y., Park, T., Akagbosu, B., Zhao, Z., Lo, Y., Shibu, G., Fisher, L., Paucar Iza, Y.A., Leslie, C., et al. (2025). A wave of Thetis cells imparts tolerance to food antigens early in life. Science *389*, 268–274. https://doi.org/10.1126/science.adp0535.

57. Fu, L., Upadhyay, R., Pokrovskii, M., Chen, F.M., Romero-Meza, G., Griesemer, A., and Littman, D.R. (2025). PRDM16-dependent antigen-presenting cells induce tolerance to gut antigens. Nature *642*, 756–765. https://doi.org/10.1038/s41586-025-08982-4.

58. Rodrigues, P.F., Wu, S., Trsan, T., Panda, S.K., Fachi, J.L., Liu, Y., Du, S., de, O.S., Antonova, A.U., Khantakova, D., et al. (2025). Rorgammat-positive dendritic cells are required for the induction of peripheral regulatory T cells in response to oral antigens. Cell *188*, 2720–2737.

59. Esterházy, D., Loschko, J., London, M., Jove, V., Oliveira, T.Y., and Mucida, D. (2016). Classical dendritic cells are required for dietary antigen-mediated induction of peripheral T_{reg} cells and tolerance. Nat. Immunol. *17*, 545–555. https://doi.org/10.1038/ni.3408.

60. Campos Canesso, M.C., de Castro, T.B.R., Nakandakari-Higa, S., Lockhart, A., Luehr, J., Bortolatto, J., Parsa, R., Esterházy, D., Lyu, M., Liu, T.T., et al. (2025). Identification of antigen-presenting cell-T cell interactions driving immune responses to food. Science *387*, eado5088. https://doi.org/10.1126/science.ado5088.

61. Akagbosu, B., Tayyebi, Z., Shibu, G., Paucar Iza, Y.A., Deep, D., Parisotto, Y.F., Fisher, L., Pasolli, H.A., Thevin, V., Elmentaite, R., et al. (2022). Novel antigen-presenting cell imparts Treg-dependent tolerance to gut microbiota. Nature *610*, 752–760. https://doi.org/10.1038/s41586-022-05309-5.

62. Mazmanian, S.K., Liu, C.H., Tzianabos, A.O., and Kasper, D.L. (2005). An immunomodulatory molecule of symbiotic bacteria directs maturation of the host immune system. Cell *122*, 107–118. https://doi.org/10.1016/j.cell.2005.05.007.

63. Wu, H.J., Ivanov, I.I., Darce, J., Hattori, K., Shima, T., Umesaki, Y., Littman, D.R., Benoist, C., and Mathis, D. (2010). Gut-residing segmented filamentous bacteria drive autoimmune arthritis via T helper 17 cells. Immunity *32*, 815–827. https://doi.org/10.1016/j.immuni.2010.06.001.

64. Lee, Y.K., Menezes, J.S., Umesaki, Y., and Mazmanian, S.K. (2011). Proinflammatory T-cell responses to gut microbiota promote experimental autoimmune encephalomyelitis. Proc. Natl. Acad. Sci. USA *108*, 4615–4622. https://doi.org/10.1073/pnas.1000082107.

65. Sivan, A., Corrales, L., Hubert, N., Williams, J.B., Aquino-Michaels, K., Earley, Z.M., Benyamin, F.W., Lei, Y.M., Jabri, B., Alegre, M.L., et al. (2015). Commensal Bifidobacterium promotes antitumor immunity and facilitates anti-PD-L1 efficacy. Science *350*, 1084–1089. https://doi.org/10.1126/science.aac4255.

66. Lin, W., Haribhai, D., Relland, L.M., Truong, N., Carlson, M.R., Williams, C.B., and Chatila, T.A. (2007). Regulatory T cell development in the absence of functional Foxp3. Nat. Immunol. *8*, 359–368. https://doi.org/10.1038/ni1445.

67. Gavin, M.A., Rasmussen, J.P., Fontenot, J.D., Vasta, V., Manganiello, V.C., Beavo, J.A., and Rudensky, A.Y. (2007). Foxp3-dependent programme of regulatory T-cell differentiation. Nature *445*, 771–775. https://doi.org/10.1038/nature05543.

68. Zemmour, D., Charbonnier, L.M., Leon, J., Six, E., Keles, S., Delville, M., Benamar, M., Baris, S., Zuber, J., Chen, K., et al. (2021). Single-cell analysis of FOXP3 deficiencies in humans and mice unmasks intrinsic and extrinsic $CD4^+$ T cell perturbations. Nat. Immunol. *22*, 607–619. https://doi.org/10.1038/s41590-021-00910-8.

69. Lio, C.W.J., and Hsieh, C.S. (2008). A two-step process for thymic regulatory T cell development. Immunity *28*, 100–111. https://doi.org/10.1016/j.immuni.2007.11.021.

70. Abdullah, L., Emiliani, F.E., Vaidya, C.M., Stuart, H., Musial, S.C., Kolling, F.W., Obar, J.J., Rosato, P.C., Ackerman, M.E., Song, L., et al. (2025). The endogenous antigen-specific CD8+ T cell repertoire is composed of unbiased and biased clonotypes with differential fate commitments. Immunity *58*, 601–615.e9. https://doi.org/10.1016/j.immuni.2025.02.001.

71. Rudnitsky, A., Oh, H., Margolin, M., Dassa, B., Shteinberg, I., Stoler-Barak, L., Shulman, Z., and Kedmi, R. (2025). A coordinated cellular network regulates tolerance to food. Nature *644*, 231–240. https://doi.org/10.1038/s41586-025-09173-x.

72. Sun, I.H., Qualls, A.E., Yin, H.S., Wang, J., Arvedson, M.P., Germino, J., Horner, N.K., Zhong, S., Du, J., Valdearcos, M., et al. (2025). RORγt eTACs mediate oral tolerance and Treg induction. J. Exp. Med. *222*, e20250573. https://doi.org/10.1084/jem.20250573.

73. Yang, Y., Torchinsky, M.B., Gobert, M., Xiong, H., Xu, M., Linehan, J.L., Alonzo, F., Ng, C., Chen, A., Lin, X., et al. (2014). Focused specificity of intestinal TH17 cells towards commensal bacterial antigens. Nature *510*, 152–156. https://doi.org/10.1038/nature13279.

74. Bettelli, E., Carrier, Y., Gao, W., Korn, T., Strom, T.B., Oukka, M., Weiner, H.L., and Kuchroo, V.K. (2006). Reciprocal developmental pathways for the generation of pathogenic effector TH17 and regulatory T cells. Nature *441*, 235–238. https://doi.org/10.1038/nature04753.

75. Kiner, E., Willie, E., Vijaykumar, B., Chowdhary, K., Schmutz, H., Chandler, J., Schnell, A., Thakore, P.I., LeGros, G., Mostafavi, S., et al. (2021). Gut $CD4^+$ T cell phenotypes are a continuum molded by microbes, not by T_H archetypes. Nat. Immunol. *22*, 216–228. https://doi.org/10.1038/s41590-020-00836-7.

76. Butler, A., Hoffman, P., Smibert, P., Papalexi, E., and Satija, R. (2018). Integrating single-cell transcriptomic data across different conditions, technologies, and species. Nat. Biotechnol. *36*, 411–420. https://doi.org/10.1038/nbt.4096.

STAR★METHODS

KEY RESOURCES TABLE

REAGENT or RESOURCE	SOURCE	IDENTIFIER
Antibodies		
Anti-mouse CD4, BV605	BioLegend	Cat# 100547; RRID: AB_11125962
Anti-mouse TCRβ, BUV737	BD	Cat# 612821; RRID: AB_2870145
Anti-mouse Thy1.1, APC-Cy7	BioLegend	Cat# 202520; RRID: AB_2303153
Anti-mouse FoxP3, PE-Cy7	eBioscience	Cat# 25-5773-82; RRID: AB_891552
Anti-mouse RORγ, BV786	BD	Cat# 564723; RRID: AB_2738916
Anti-mouse Helios, PB	BioLegend	Cat# 137220; RRID: AB_10690535
Anti-mouse TCR Vβ5.1, 5.2, FITC	BioLegend	Cat# 139513; RRID: AB_2750132
Anti-mouse TCR Vβ3, BUV395	BD	Cat# 743418; RRID: AB_2741491
Anti-mouse TCR Vβ2, AF647	BioLegend	Cat# 127910; RRID: AB_1089254
Anti-mouse TCR Vβ8.3, FITC	BioLegend	Cat# 156305; RRID: AB_2800701
Anti-mouse TCR Vβ8.3, PE	BioLegend	Cat# 156303; RRID: AB_2800699
Anti-mouse TCR Vα2, PERCP-CY5.5	BioLegend	Cat# 127813; RRID: AB_1186118
Anti-mouse TCR Vβ11, APC	BioLegend	Cat# 125913; RRID: AB_2800608
Anti-mouse TCR Vβ 8.1, 8.2, PE	BioLegend	Cat# 140103; RRID: AB_10641144
Anti-mouse TCR Vβ12, Percp-ef710	ThermoFisher	Cat# 46-5798-80; RRID: AB_10852552
Anti-mouse TCR Vα11.1, 11.2, FITC	BD	Cat# 553222; RRID: AB_394717
Anti-mouse TCR Vα8.3, FITC	BioLegend	Cat# 127705; RRID: AB_1186078
Anti-mouse CD25, PE	BioLegend	Cat# 102008; RRID: AB_312857
Anti-mouse CD45.2, PE-Cy7	BioLegend	Cat# 109830; RRID: AB_1186098
TotalSeq-C anti-mouse hashtags	BioLegend	Cat# 155861; RRID: AB_2800693, Cat# 155863; RRID: AB_2800694, Cat# 155865; RRID: AB_2800695, Cat# 155867; RRID: AB_2800696, Cat# 155869; RRID: AB_2800697, Cat# 155871; RRID: AB_2819910, Cat# 155873; RRID: AB_2819911, Cat# 155885; RRID: AB_2922483, Cat# 155887; RRID: AB_2922484, Cat# 155889; RRID: AB_2924484, Cat# 155891; RRID: AB_2924485, Cat# 113931; RRID: AB_2941396, Cat# 113929; RRID: AB_2941395, Cat# 155893; RRID: AB_2927982, Cat# 155895; RRID: AB_2927981
Chemicals, peptides, and recombinant proteins		
Fixable Viability Dye eFluor506	ThermoFisher	Cat# 65-0866-14
Recombinant human IL-2	peprotech	Cat# 200-02
Recombinant Mouse IL-7 (carrier-free)	BioLegend	Cat# 577804
Streptomycin sulfate	Sigma-Aldrich	Cat# S6501
LB Agar	Miller BD	Cat# 244520
LB Broth	Miller BD	Cat# 244620
BD BBL™ Brucella Agar with 5% Sheep Blood	Hardy Diagnostics	Cat# A30
Dispase	ThermoFisher	Cat# 17105041
Collagenase type II	Gibco	Cat# 17101015
EDTA	VWR	Cat# BDH7830-1

(*Continued on next page*)

Continued

REAGENT or RESOURCE	SOURCE	IDENTIFIER
DL-Dithiothreitol	Sigma	Cat# D9163-25G
Phosphate-buffered saline (PBS, 10X), pH 7.6	ThermoFisher	Cat# J62692.K2
UltraPure™ 1M Tris-HCl, pH 8.0	Invitrogen	Cat# 15568025
RPMI 1640	Gibco	Cat# 11875093
Penicillin-streptomycin	ThermoFisher	Cat# 15140122
Sodium pyruvate	Gibco	Cat# 11360070
HEPES	Invitrogen	Cat# 15630-080
β-mercaptoethanol	Gibco	Cat# 21985-023
Benzonase	Millipore Sigma	Cat# 70-664-3
OptiPrep	StemCell Technologies	Cat# 07820
Polyethylenimine	Polysciences	Cat# 23966
Critical commercial assays		
Dynabeads® Mouse T-Activator CD3/CD28	Invitrogen	Cat# 11452D
Dynabeads™ Untouched™ Mouse CD4 Cells Kit	Invitrogen	Cat# 11415D
FoxP3 / Transcription Factor Staining Buffer Set	eBioscience	Cat# 00-5523-00
123count eBeads	Invitrogen	Cat# 01-1234-42
Amicon Ultra-15 Centrifugal Filter Unit	Millipore	Cat# UFC905024
Nalgene 0.45um PES filter	ThermoFisher	Cat# 165-0045
Coulter OptiSeal Tube	Beckman	Cat# 361625
Diet: 5058 PicoLab® Mouse Diet 20	LabDiet	N/A
Diet: amino acid- based diet	LabDiet	Cat# A12450KR
Diet: 5010 Laboratory Autoclavable Rodent Diet	LabDiet	N/A
Gibson Assembly® Master Mix	NEB	Cat# E2611S
BmgBI	NEB	Cat# R0628S
PflMI	NEB	Cat# R0509S
Chromium GEM-X Single Cell 5' Reagent Kits v2	10X Genomics	PN-1000263
GEM-X Universal 5' Gene Expression v3 4-plex	10X Genomics	PN-1000780
GEM-X OCM 5' Chip Kit v3 4-plex 2 chips	10X Genomics	PN-1000748
Dual Index Kit TT Set A 96 rxns	10X Genomics	PN-1000215, PN-1000242
Library Construction Kit C 16 rxns	10X Genomics	PN-1000694
Deposited data		
scRNA-seq	This paper	GSE301231
RORγ+ Treg signatures	Hanna. B. at al	GSE196337
Bacterial and virus strains		
E.coli Nissle	Dr. Dennis Kasper	N/A
Clostridium ramosum	Dr. Dennis Kasper	N/A
NEB Stable Competent E.coli	NEB	Cat# C3040I
Experimental Models: Cell lines		
293T	ATCC	Cat# CRL-3216
Experimental Models: Organisms/Strains		
Mouse: C57BL/6J	Jackson Laboratory	JAX# 000664
Mouse: Cas9 knockin	Jackson Laboratory	JAX# 026179
Mouse: B6. FoxP3-IRES-eGFP	Dr. Vijay K. Kuchroo	N/A

(*Continued on next page*)

Continued

REAGENT or RESOURCE	SOURCE	IDENTIFIER
Mouse: congenic Thy1.1 strain	Jackson Laboratory	JAX# 000406
Mouse: HH7-2tg transgenic mice	Dr. Dan Littman	N/A
Mouse: BθOM transgenic mice	Dr. Gérard Eberl	N/A
Mouse: *Clec9a*^{cre}	Dr. Chrysothemis C. Brown	N/A
Mouse: *Rorc*^{cre}	Dr. Chrysothemis C. Brown	N/A
Mouse: *H2-Ab1*$^{fl/fl}$	Dr. Chrysothemis C. Brown	N/A
Germ Free C57BL/6J mice	GF C57BL/6 colony housed in the animal facility at HMS	N/A
Recombinant DNA		
pHelper	Dr. Justin Eyquem	N/A
pArk313	Dr. Justin Eyquem	N/A
U6/gTrac-Trbc-TCR (24 in total)	This paper	N/A
Software and algorithms		
FlowJo v10	FlowJo, LLC	https://www.flowjo.com/
Prism10	GraphPad	https://www.graphpad.com/
R version 4.4.1	The R Foundation	https://www.r-project.org/
Seurat_5.1.0	N/A	https://satijalab.org/seurat/
Cell Ranger v7.1.0.	10X Genomics	N/A

METHOD DETAILS

Mice

Foxp$^{IRES\text{-}GFP}$/B6,[74] C57BL/6J (JAX: 000664), congenic Thy1.1 strain (JAX: 000406), Rosa26-*Cas9* knock-in mice (JAX: 026179), *Clec9a*^{cre}, *Rorc*^{cre}, *H2-Ab1*$^{fl/fl}$[61] mice were maintained in our colony at HMS or MSK. HH7-2tg[17] transgenic mice were obtained from the Littman lab, BθOM[8] mice were reconstituted from sperm from the MMRRC repository. All mice are under B6 background. Mice were housed under specific pathogen-free conditions. Gnotobiotic C57BL/6J mice were maintained at the Harvard Medical School Gnotobiotic Core Facility. SPF mice were under 5058 chow (LabDiet), gnotobiotic mice were fed on 5010 chow (LabDiet), or AFD (LabDiet, A12450KR) where indicated. The ingredients of each diet are in Table S4. All experimentation was performed following HMS IACUC protocol IS00001257, and MSK (IACUC protocol 21-05-007). Both male and female were used for all experiments. 7-12-week-old adult mice were used for most experiments, except *MHCII*$^{\Delta ROR\gamma}$ and *MHCII*$^{\Delta Clec9a}$ hosts.

TCRs

TCR used in this study were identified in colonic Treg and Tconv CD4$^+$ cells from SPF or monocolonized mice, as described in Ramanan et al.,[29] as detailed in Figure S1.

TCR editing of primary CD4$^+$ T cells

TCR editing was performed largely according to Nyberg et al.[36] TCRs of interest were cloned as bi-cistronic cassette into the Ark313 vector, high-titer AAV stocks were prepared and used to infect CD4$^+$ T cells from Cas9-exprssing transgenic mice, resulting in inactivation of both endogenous TCR loci and insertion of the recombinant TCR into the *Trac* locus for proper expression in T cells.

TCR cloning into AAV vectors

To generate TCR-targeting constructs for site-specific integration at the *Trac* locus, plasmids were derived by cloning an expression cassette for each TCR into pAAV-U6/gTrac-Trac-OT-I.[36] designed to contain 500bp homology arms targeting *Trac* exon 1 flanking the intended knock-in region, with a U6 promoter-driven sgRNA targeting *Trac* for cleavage (UAUGGAUUCCAAGAGCAAUG) at the 5' end, and a U6 promoter-driven sgRNA targeting *Trbc* (CUGGUGGGUGAAUGGCAAGG) for knockout at the 3' end. The transgene cassette contained a P2A linker 1, TCRβ VDJ region coding sequences (starting from the first methionine codon of the V region gene), directly followed by *Trbc* sequences, P2A linker 2, TCRα VJ region coding sequences (starting from the first methionine codon from variable region sequencing), and partial TCRα constant region beginning with amino acid sequence "IQNPEP" which, in combination with the right homology arm (RHA), restores the complete endogenous TRAC coding sequence while forming a functional TCR of the intended specificity. Both *Trac* and *Trbc* sequences were codon-optimized to prevent re-cutting by their respective sgRNAs and eliminate sequence homology with endogenous genes to prevent recombination. Two distinct P2A ribosomal skipping sequences were used to prevent recombination between linker regions during cloning and integration. Individual TCRs were synthesized as double-stranded DNA and assembled using Gibson assembly and restriction enzyme cloning, with the AAV backbone generated

exclusively through restriction enzyme cloning using BmgBI and PflMI sites to preserve AAV inverted terminal repeat integrity and avoid PCR-induced mutations that could compromise AAV packaging efficiency.

Viral preparations

AAV were produced using HEK293T cells. HEK293T cells were seeded in 150 mm dishes and transfected at approximately 70–80% confluency using polyethylenimine (PEI; Polysciences #23966). Each dish was transfected with 6 μg of AAV cargo plasmid containing the transgene cassette flanked by AAV2-ITRs, 8 μg of Ark313 capsid plasmid, and 11 μg of adenoviral helper plasmid providing essential adenoviral helper functions for AAV production. Transfection was performed in 200 μL of PEI per plate, and cells were incubated at 37°C with 5% CO_2. After 72 hours, viral particles were harvested from both the cell lysate and supernatant.

Cells were collected in AAV lysis buffer (50 mM Tris, 150 mM NaCl) and subjected to three rounds of freeze-thaw cycles to lyse the cells and release viral particles. Lysates were treated with Benzonase (25 U/mL; Millipore Sigma #70-664-3) at 37°C for 1 hour to degrade residual nucleic acids. Crude lysates were clarified by centrifugation at 3,000 × g for 10 minutes at 4°C, and viral particles were purified using iodixanol (OptiPrep, STEMCELL Technologies #07820) gradient ultracentrifugation. Following centrifugation, the AAV-containing fraction was extracted, dialyzed against PBS to remove iodixanol, and concentrated using Amicon Ultra-15 centrifugal filter units (Millipore Sigma #UFC910024).

AAV titers were determined by qPCR using DNase I (NEB #B0303S)-treated and Proteinase K (Qiagen #1114886)-digested AAV samples. qPCR was performed with SsoFast Eva Green Supermix (Bio-Rad #1725201) on a StepOnePlus Real-Time PCR System (Applied Biosystems #4376600) using primers targeting the viral genome. Relative viral genome quantities were estimated by comparison to a standard curve generated from serial dilutions of a plasmid of known concentration.

Editing of primary CD4⁺ cells

T cells were isolated from the spleens of Cas9-expressing transgenic mice. Spleens were mechanically disrupted and passed through a 40 μm cell strainer to obtain a single-cell suspension. Red blood cells were lysed using ammonium-chloride-potassium (ACK) lysis buffer, followed by washing with PBS. CD4⁺ T cells were enriched using the Dynabeads Untouched Mouse CD4 Cells Kit (Invitrogen #11416D), according to the manufacturer's protocol. Purified T cells were activated with Dynabeads Mouse T-Expander CD3/CD28 (Gibco #11452D) and 200 U/mL recombinant human IL-2 (PeproTech #200-02) for 1 day. Activated T cells were resuspended at a density of 2×10^6 cells/mL and incubated with AAV. The following day, the AAV-containing medium was replaced with fresh culture medium, and cells were maintained under standard culture conditions. Two days later, cells were resuspended in resting culture medium with 10 ng/mL IL-7 (BioLegend # 577802). Four days later, transduction efficiency and FoxP3 expression was assessed by flow cytometry before they were transferred into host mice.

In vitro screening of antigen reactivity

Antigen sources included:

1. Heat killed bacteria. *E. coli Nissle* or *C. ramosum* were resuspended in PBS at the concentration of OD600=1, and then were heat treated at 75 °C for 1 hour. 5 μL of this suspension was used for each co-culture in a total culture volume of 150 μL.
2. Gut contents. Colon and cecum contents from indicated mice were diluted in PBS, vortex mixed, homogenized, filtered through 70 μm mesh, adjusted to concentration of OD600=1, and heat treated at 75 °C for 1 hour to kill all microbes. 5 μL of this suspension was used for each co-culture in a total culture volume of 150 μL.
3. Protein extracts. Whole 5058 chow or individual chow components (LabDiet) were dissociated in extraction media (600 mM KCl, 20 mM Tris-Cl pH 7.8, 10% Glycerol, and 1x cOmplete protease inhibitor in ddH2O). Colon contents were similarly processed and bacteria were removed by spin down at 2000g for 10 mins to extract digested food antigens. All samples then underwent 5 freeze thaw cycles alternating between dry ice and 37°C water bath. Samples were centrifuged for at 2000g for 10 minutes at 4°C. Supernatant was diluted into prechilled (-20°C) acetone at a 1:4 ratio, mixed thoroughly and incubated at -20°C for 30-60 minutes. Samples were centrifuged at 15,000g for 10min at 4°C. Supernatant was discarded and the remaining protein pellet was resuspended in DMEM without phenol red with 20 mM HEPES. Resuspended samples were centrifuged at 50g for 5 min at 4°C to remove any insoluble components. Protein concentration of the soluble fraction was measured by BCA assay. 20 μg/mL protein extracts were used for co-cultures.

T-APC coculture

To isolate APCs, spleens from B6 mice were digested with 0.5 mg/mL collagenase D and 0.1 mg/mL DNase for 30 min at 37°C. Single-cell suspensions were prepared, and CD11c⁺ cells were enriched by surface staining of CD11c-biotin antibody followed by Streptavidin MicroBeads (Miltenyi Biotec #130-048-101) treatment. Alternatively, whole adherent spleen cells were used as APCs. Single-cell spleen suspensions were plated onto 60 mm culture dishes for 90 min to allow APC to adhere. Non-adherent cells were removed by washing several times with complete medium. Fresh media were added for another hour, and adherent cells were then eluted by gentle pipetting. Similar results were gotten and combined from both methods. Enriched APCs were pre-activated with 100 ng/mL LPS with indicated antigen sources (20 μg/mL protein extracts or 5 μL heat killed bacteria or gut content in 150 μL total culture volume) overnight. Then APCs were co-cultured with TCR edited T cells at 1:1 ratio and co-responding antigens for 1.5 day. CD25 or Nur77 expression on TCRb⁺ cells were analyzed to indicated cell activation.

Gene inactivation by electroporation of Cas9/gRNA complexes

CRISPR–Cas9 ribonucleoproteins (crRNPs) were prepared by incubating Cas9 protein with crRNA-tracrRNA duplexes, a pre-complexed two part-system with gRNA functionality. Five different predesigned crRNAs (CGTTGACAAGGGGGTTCTTC; ATGGA TGACGCATTGGTACT; CTGTGCGTTGCAAACAGTGT; GGGGCAAATCAGGGTAACGG; CCCCACCAGGTGATCATTCA) targeting exon 2, 3, 4 and 6 of *Il6ra* were selected from Custom Alt-R CRISPR-CAS9 guide RNA service (IDT), and the common scaffold trans-activating RNA (tracrRNA) were obtained from IDT (Cat# 1072533). Non-targeting control crRNAs (IDT, Cat # 1072544, 1072545) were used as negative controls. The crRNA and tracrRNA oligos were mixed well in equimolar concentration to reach a final duplex concentration of 40 μM, and incubated at 37 °C for 30 mins. The crRNA-tracrRNA duplex were then mixed with Cas9-NLS (Macrolab, UC Berkeley) to achieve a duplex/Cas9 protein ratio of 2:1. For example, for 100 μL electroporation reaction, 11.25 μg Cas9 weas incubated with 0.4 nanomole of crRNA-tracrRNA duplexes. The complexes were allowed to form for 15 mins at 37 °C, and kept on ice before use (less than 30 minutes).

CD4$^+$ T cells were enriched from Thy1.2-Cas9 or Thy1.1-Cas9 (CD45.2) mice by Dynabeads Untouched Mouse CD4 Cell Kit (Invitrogen, Cat# 11415D) per manufacturer's instructions. 12 million primary CD4$^+$ T cells were washed with Ca/Mg free PBS and centrifuged at 500g for 5 mins. The crRNPs complex were mixed gently with 100 μL electroporation solution cP4 (Lonza, V4XP-4024), incubated at room temperature for 2 mins, and cells were resuspended in this solution before transfer into Large Lonza cuvette strip. Nucleofection was then performed using Amaxa 4D-Nucleofector under X-P4 and program DS137. After electroporation, 750 μL of pre-warmed T cell culture medium supplemented with 10 ng/ml mIL7 were gently added to the cuvette containing electroporated cells. Electroporated cells were transferred into 12-well plates after 50 mins resting in 37 °C, 5% CO2 incubator, and cells underwent TCR editing 24 hours later.

Bacteria culture and colonization

Escherichia coli Nissle 1917 (Kasper lab collection) was grown overnight in Lennox Luria-Bertani (LB; BD Difco) supplemented with 100 μg/mL streptomycin at 37 °C. On the following day, *E. coli* Nissle cultures were spin down 2000xg for 5 mins and resuspended in PBS to an OD600=1. To colonize SPF mice with *E. coli* Nissle, adult SPF mice were gavaged with 20 mg streptomycin at day -1 and day 4 relative to cell transfer, and 100 μL *E. coli* Nissle resuspension was gavaged on day 0 and day 5. Germ free C57BL/6 host mice were inoculated with 100 μL *E. coli* Nissle suspensions, and maintained in Iso Positive Individually Ventilated cages. Two weeks after colonization, mice were used for cell transfer. For experiments using *MHCII*$^{\Delta ROR\gamma}$ and *MHCII*$^{\Delta Clec9a}$ hosts, neonate mice were gavaged with *E. coli* Nissle twice at d10 and d15, and were transferred cells between d18-d26.

Clostridium ramosum (Kasper lab collection) was cultured on Brucella Blood Agar with Hemin and Vitamin K (Hardy Diagnostics #A30) under anaerobic conditions (80% N_2, 10% H_2, 10% CO_2) at 37°C in an anaerobic chamber for one day. All colonies from one plate were resuspended in 1.5 mL PBS for oral gavage. Germ free C57BL/6 host mice were inoculated with 100 μL *C. ramosum* suspensions, and maintained in Iso Positive Individually Ventilated cages. Two weeks after colonization, mice were used for cell transfer.

Helicobacter hepaticus was a kind gift from the Littman lab. It was thawed from Brucella broth and glycerol aliquots, resuspended in Brucella broth and cultured on TSA+5% sheep blood for 3 days anaerobically in an Embrient hypoxia chamber filled with O2-less gas (Airgas). It was then picked from the plate using cotton swabs and resuspended in Brucella broth+20% glycerol aliquots (OD600= >2) that were frozen in liquid nitrogen and thawed for gavage (200 μL).

Bacteroides thetaiotamicron was obtained from the Martens lab (U. of Michigan). It is grown on Brucella H+K agar for between 2 and 5 days. Multiple colonies are harvested and suspended in TYG medium, spun down and resuspended in TYG at OD600=1 to 1.5 before gavage (200 μL).

Cell transfers and donor cell assessment

Unless otherwise specified, 100K-200K TCR edited Thy1.1/Cas9 cells were transferred into B6 mice via intravenous injection. In most experiments, tissues were analyzed ten days post cell transfer, except for Figures 1E and 1F (one day) and Figure 5 (6-10 weeks). The analyzed tissues included spleen, subcutaneous lymph nodes (scLN), small intestine- and colon-draining mesenteric LNs (smLN and cmLN), colon and ileum lamina propria. Donor cells were identified as live/dead$^-$CD4$^+$Thy1.1$^+$. Among them, TCR$^-$ cells were negative for TCRβ expression. TCR edited cells were positive for specific antibodies targeting the introduced TCR variable region, while non-edited cells were TCRβ$^+$ but negative for edited TCR variable regions. For transgenic cell transfers, HH7-2tg and BθOM Tconv cells were sorted from the spleen as TCRβ$^+$CD4$^+$ FoxP3-GFP$^-$ and 100K cells were transferred by intravenous injection.

Lymphocyte isolation from tissues

Colon and ileum (removed Peyer's Patches) were cleaned and treated with RPMI containing 1 mM DTT, 20 mM EDTA and 2% FBS at 37°C for 20 min to remove epithelial layers, minced and dissociated in collagenase solution in RPMI containing 1.5 mg/mL collagenase II (Gibco # 17101015), 0.5 mg/mL dispase (Gibco #17105041) and 2% FBS, with constantly stirring at 37°C for 40 min. Single cell suspensions were then filtered through 40 μm strainers and washed with RPMI solution. Lymph nodes and spleens were mechanically disrupted and filtered through 40 μm cell strainer to get single-cell suspensions. Red blood cells in the spleen were lysed with ACK lysing buffer (Gibco #A10492-01).

Flow cytometry

Single-cell suspensions were stained with surface markers live/dead, CD4, TCRβ, CD25, indicated antibodies for variable regions of TCRα or TCRβ at 4°C for 20 min. For intracellular staining, cells were fixed in Fix/Perm buffer (eBioscience) at room temperature for 1 hour, followed by permeabilization in permeabilization buffer at room temperature for 1 hour in the presence of antibodies FoxP3, Helios, and RORγ. Cells were recorded by a Symphony flow cytometer (BD Biosciences) and analysis was performed with FlowJo software.

scRNA-seq pTreg profiling

Sample preparation and sequencing

scRNA-seq experiments were performed and analyzed as previously described.[75] TCR edited cells (*Cas9/FoxP3^{GFP}*) were transferred into CD45.1 hosts to analyze donor derived pTreg and Tconv cells. T cells infected with AAV carrying an early stopped codon in the TCR gene were used for TCR negative control (no TCR expression was confirmed). Cells subjected to mock infection (same in vitro culture procedure without virus) served as non-edited controls. For each TCR editing group, cells from 5-7 mice were pooled together to get sufficient cell numbers. Host cells from the same recipient mice, or FoxP3$^+$ and FoxP3$^-$ cells from an extra *FoxP3^{GFP}* mice were used for references.

Ten days post cell transfer, CD4$^+$ T cells were enriched from mLN single cell suspensions before surface staining. Cells were then stained with antibodies against CD4, TCRβ, CD45.2, CD25, TCRVβ5 (TF2.2), TCRVα2 (TF2.7), TCRVβ8.3 (TF2.6), TCRVβ12 (TM3.5), TCRVβ2 (TM2.3), TCRVα11 (TM1.2), TCRVβ5 (TS2.1), TCRVβ11 (TS2.3) and 4′,6-diamidino-2-phenylindole (DAPI) as a viability dye, along with hashtag antibodies (Biolegend, TotalSeq-C anti-mouse hashtags) for each population in staining buffer (DMEM, 5% fetal calf serum) for 20 min at 4°C in the dark. Indicated DAPI-CD4$^+$ populations (CD45.2$^+$TCRV$^+$GFP$^+$ for donor pTregs, CD45.2$^+$TCRV$^+$GFP$^-$ for donor Tconv, CD45.2$^+$TCRβ$^-$ for TCR$^-$, CD45.2$^+$TCRβ$^+$ for non-edited; CD45.2-GFP$^+$ or CD25hi for reference Treg cells, CD45.2-GFP$^-$ or CD25low for reference Tconv cells) were sorted with a FACSAria III. Samples were pooled together, centrifuged, and resuspended in 2% Fetal Calf Serum (FCS).

Encapsulation was done on the 10X Chromium Controller (10X Genomics). Libraries were prepared using Chromium Single Cell 5′ Reagents Kit v2 according to the manufacturer's protocol (CG000330, Figure 5), or GEM-X Universal 5' Gene Expression v3 4-plex" and "Chromium GEM-X Single Cell 5' Reagent Kits v3 with Feature Barcode technology for Cell Surface Protein" according to the manufacturer's protocol (CG000770, CG000734, Figure 4). After cDNA amplification, the smaller fragments containing the TotalSeq-C–derived cDNA were purified and saved for feature barcode library construction. The larger fragments containing transcript-derived cDNA were saved for gene expression library construction. Libraries were sequenced together on the Illumina Novaseq X.

Data analysis

scRNA-seq data were processed using the standard CellRanger pipeline (10X Genomics), where RNA and Hashtag oligo (HTO) counts were obtained together through the cellranger count function. Data were analyzed in R using the Seurat package.[76] HTOs were assigned to cells using the HTODemux function, and cells assigned doublets or negatives were eliminated from analysis. Cells with fewer than 1000 unique molecular identifiers (UMIs) or 400 genes and more than 2500 UMIs, 10,000 genes, and 5% of reads mapped to mitochondrial genes were also excluded from the analysis. Dimensionality reduction, visualization, and clustering analysis were performed in Seurat using the NormalizeData, ScaleData, FindVariableGenes, RunPCA, FindNeighbors (dims=1:20), RunUMAP (dims=1:20), and FindClusters functions. Cluster identity was determined based on expression of key marker genes (Figures 4B and S5B). Differentially expressed genes (DEGs) were obtained using the FindMarkers function, with the cutoff based on absolute avg_log2FC >1, adjusted P value < 0.05, and a pct >10%.

QUANTIFICATION AND STATISTICAL ANALYSIS

Data were shown as mean ± standard error of the mean. Statistical significance was determined using one sample t-test for Figure 1F, two-tailed t.test (paired or unpaired as indicated) for two groups, and a Fisher test for determining gene signature significance in volcano plots. Statistical significance was defined as $P < 0.05$. The level of significance in all graphs is represented as follows: * for $P < 0.05$, ** for $P < 0.01$, *** for $P < 0.001$. Statistics were computed in GraphPad Prism or R.

Immunity, Volume *59*

Supplemental information

TCR origin and specificity to environmental or self-antigens on distinct antigen-presenting cells determine peripheral Treg cell differentiation

Xinxin Chi, Charlotte H. Wang, Yollanda Franco Parisotto, William A. Nyberg, Vanja Cabric, Adelaide Gelineau, Yi Cao, David L. Owen, Jonas Ambjörnsson, Diane Mathis, Justin Eyquem, Chrysothemis C. Brown, and Christophe Benoist

Immunity, Volume *59*

Supplemental information

TCR origin and specificity to environmental or self-antigens on distinct antigen-presenting cells determine peripheral Treg cell differentiation

Xinxin Chi, Charlotte H. Wang, Yollanda Franco Parisotto, William A. Nyberg, Vanja Cabric, Adelaide Gelineau, Yi Cao, David L. Owen, Jonas Ambjörnsson, Diane Mathis, Justin Eyquem, Chrysothemis C. Brown, and Christophe Benoist

SUPPLEMENTARY FIGURE LEGENDS

Fig. S1. Summary table of selected TCR information, related to Figure 1. Amplified clonotypes were picked from Tconv, RORγ^{+}Treg, Helios^{+}Treg or RORγ^{-}Helios^{-} (DN) Treg populations from gnotobiotic mice monocolonized by *C. ramosum* or *E. coli Nissle* [29]. Numbers indicate the number of times each clonotype was recovered.

Fig. S2. pTreg generation is consistent in different conditions, related to Figure2. (A) Representative FACS plot (left) and pooled statistic data (right) of FoxP3 expression in TCR-edited cells before adoptive transfer. **(B-F)** CD4^{+} donor cells were transferred into indicated hosts for ten days. **(B)** Representative flow cytometric plots showing gating strategy to identify TCR-negative, TCR-edited and non-edited donor cells. **(C)** Representative flow cytometric plots of donor cell distribution in different tissues. **(D)** summary of FoxP3 expression in TCR-negative and non-edited cells. **(E)** Quantification of FoxP3 expression of TM3.5 and TM2.3 TCR-edited cells in EcN colonized gnotobiotic or SPF hosts. **(F)** 37.5K or 150K TCR edited cells were transferred into SPF hosts for 10 days. Quantification of FoxP3^{+}% and FoxP3^{+} cell number in indicated tissues. **(G)** Quantification of FoxP3 expression of TS2.1-TS2.5 TCR-edited cells in SPF mice under chow or AFD, or GF mice under chow or AFD diet. **(H)** Upper: Schematic illustrating experimental procedures for transferring naïve CD4^{+} TCR transgenic cells into hosts with or without corresponding bacteria colonization. Lower: Quantification of FoxP3 expression of BθOM or HH7-2 TCR transgenic CD4 T cells in B. theta or H. hepaticus colonized or control mice respectively. Each dot represents one mouse. Results are pooled from multiple independent experiments.

Fig. S3. Time course of pTreg generation, related to Figure2. TCR-edited CD4^{+} donor cells were transferred into B6 hosts and analyzed at indicated time point. **(A)** Representative FACS plots of FoxP3 and RORγ expression in TF2.5 TCR-edited cells. **(B)** Summary plots of FoxP3 expression. Results are pooled from two independent experiments. Two to three mice were used per TCR. Only samples with more than 10 cells for each TCR-edited population within a given tissue were included in the analysis.

Fig. S4. Helios expression levels in donor and host Tregs, related to Figure3. TCR-edited $CD4^+$ donor cells were transferred into B6 hosts and analyzed ten days later. Summary plots of Helios MFI in TF2.2- and TS2.3-pTregs and corresponding host Tregs. Results are pooled from multiple independent experiments. Each dot pair represent one mouse. Statistical significance determined by paired Student's t test, $^{**}P < 0.01$, $^{***}P < 0.001$.

Fig. S5. scRNA-seq reveals unique transcriptome of different TCR guided pTregs, related to Figure4.

Cells isolated from mLNs 10 days after adoptive transfer were analyzed by scRNA-seq analysis. Three TCRs were used: TM3.5 (EcN-reactive), TS2.3 (self-reactive) and TF2.2 (food-reactive) **(A)** UMAP of scRNA-seq data encompassing all groups, annotation based on expression of key indicator genes **(B)** and on reference cells in C. **(C)** Position of cells from each group on the collective UMAP; experimental groups on the top row, reference groups on the bottom row, including, from left to right: donor-derived non-edited and TCR-negative Tconv, standard mLN Tconv and Treg $CD4^+$ cells from a FoxP3-GFP reporter mouse, and host Treg cells from TF2.2 and TM3.5 transfers (these contain a few Tconv cells because sorted on CD25). **(D)** UMAP plot grouping TF2.2-, TM3.5- and TS2.3-expressing pTregs. **(E)** Expression of Treg-related marker genes. The dot size represents the percentage of cells in a group that express the transcript, and the color indicates the average expression level. **(F)** Volcano plot of differentially expressed genes between TF2.2 and TS2.3 TCR-expressing pTregs. Red and blue dots represent genes highly expressed in colonic $ROR\gamma^+$ or $Helios^+$ Tregs respectively. Statistical significance of the enrichment in F was determined using Fisher's test.

Figure S1

Clone ID	Original mouse	alpha.vgene	alpha.jgene	alpha junction	beta.vgene	beta.jgene	beta junction	Act Tconv	Rorg Treg	Helios Treg	DN Treg
T01.1	Crm_mouse4.2	TRAV8D-2	TRAJ49	CATDAGYQNFYF	TRBV3	TRBJ2-5	CASSILTGGQDTQYF	11	0	0	0
TM1.3	EcN_mouse6.2	TRAV4-4-DV10	TRAJ56	CAAEATGGNNKLTF	TRBV20	TRBJ1-3	CGAGVAGNTLYF	5	0	0	0
T02.3	SPF_mouse6.1	TRAV12D-2	TRAJ31	CALSGDNNRIFF	TRBV13-3	TRBJ2-7	CASSGGGRDEQYF	0	5	0	0
TM1.1	EcN_mouse6.2	TRAV6N-7	TRAJ33	CALGSNYQLIW	TRBV15	TRBJ2-3	CASSLTGGAGAETLYF	22	0	0	0
TM1.2	EcN_mouse6.1	TRAV4D-4	TRAJ6	CAAEATGGNYKPTF	TRBV3	TRBJ2-7	CASSSRDWGGEQYF	11	0	0	0
TM2.3	EcN_mouse6.2	TRAV7-5	TRAJ39	CAVNNAGAKLTF	TRBV13-1	TRBJ1-2	CASSEGGNSDYTF	0	5	0	1
TM3.4	Crm_mouse4.1	TRAV3-1	TRAJ9	CAVSEGMGYKLTF	TRBV26	TRBJ2-4	CASSPGLSQNTLYF	1	10	0	0
TM3.5	EcN_mouse6.2	TRAV6-7-DV9	TRAJ48	CALSSNYGNEKITF	TRBV15	TRBJ1-1	CASRATGRNTEVFF	2	6	0	0
TM2.6	Crm_mouse6.1	TRAV12D-3	TRAJ26	CALSEGNNYAQGLTF	TRBV12-2+TRBV13-3	TRBJ1-2	CASVDQNSGNTLYF	0	4	0	0
TM2.7	Crm_mouse6.1	TRAV13-1	TRAJ21	CALDPLSNYNVLYF	TRBV13-1	TRBJ2-4	CASRELGDGQNTLYF	0	3	0	0
TF2.1	Crm_mouse4.2	TRAV9-1	TRAJ21	CAVSALWSNYNVLYF	TRBV13-1	TRBJ2-1	CASSPGLGGRGAEQFF	0	7	0	2
TF2.2	Crm_mouse4.2	TRAV7D-3	TRAJ13	CAVSIGGTYQRF	TRBV12-2	TRBJ2-5	CASSLGGGQDTQYF	0	0	2	2
TF3.3	multiple mouse	TRAV17	TRAJ58	CALEGQGTGSKLSF	TRBV1	TRBJ2-2	CTCSAGLGANTGQLYF	1	3	2	1
TF3.4	multiple mouse	TRAV7-5	TRAJ48	CAVSSNYGNEKITF	TRBV26	TRBJ2-1	CASSLGAEQFF	2	4	3	2
TF2.5	EcN_mouse4.1	TRAV13D-2	TRAJ4	CAHRLSGSFNKLTF	TRBV1	TRBJ2-5	CTCSAPSNQDTQYF	0	4	0	0
TF2.6	EcN_mouse6.2	TRAV7-2	TRAJ42	CAYYSGGSNAKLTF	TRBV13-1	TRBJ2-7	CASSGTGVEQYF	0	3	0	0
TF2.7	Crm_mouse4.1	TRAV14-2	TRAJ37	CAASITGNTGKLIF	TRBV3	TRBJ2-4	CASSSWGNTLYF	0	0	0	2
TF2.8	EcN_mouse3.1	TRAV7-5	TRAJ48	CAVSINYGNEKITF	TRBV26	TRBJ2-7	CASSLGAEQYF	0	0	0	2
TF2.9	SPF_mouse6.1	TRAV8D-2	TRAJ32	CATDGYGGSGNKLIF	TRBV26	TRBJ2-2	CASSRQGPNTGQLYF	0	0	0	2
TS2.1	EcN_mouse6.1	TRAV9N-4	TRAJ12	CALSRAGGYKVVF	TRBV12-2	TRBJ2-5	CASSLGGQDTQYF	0	0	0	2
TS2.2	Crm_mouse4.1	TRAV3-1	TRAJ40	CAVSEMSTGNYKYVF	TRBV26	TRBJ1-3	CASSLSGNTLYF	0	0	3	0
TS2.3	EcN_mouse4.2	TRAV4-2	TRAJ13	CEGNSGTYQRF	TRBV16	TRBJ2-1	CASSPRLGGRAEQFF	0	0	3	0
TS2.4	EcN_mouse6.2	TRAV14D-3-DV8	TRAJ9	CAASGGNMGYKLTF	TRBV20	TRBJ1-5	CGASGQGNQAPLF	0	0	3	0
TS2.5	SPF_mouse6.1	TRAV12-3	TRAJ57	CALSEQGGSAKLIF	TRBV10	TRBJ2-5	CASSWTGGRDTQYF	0	0	4	0

Figure S2

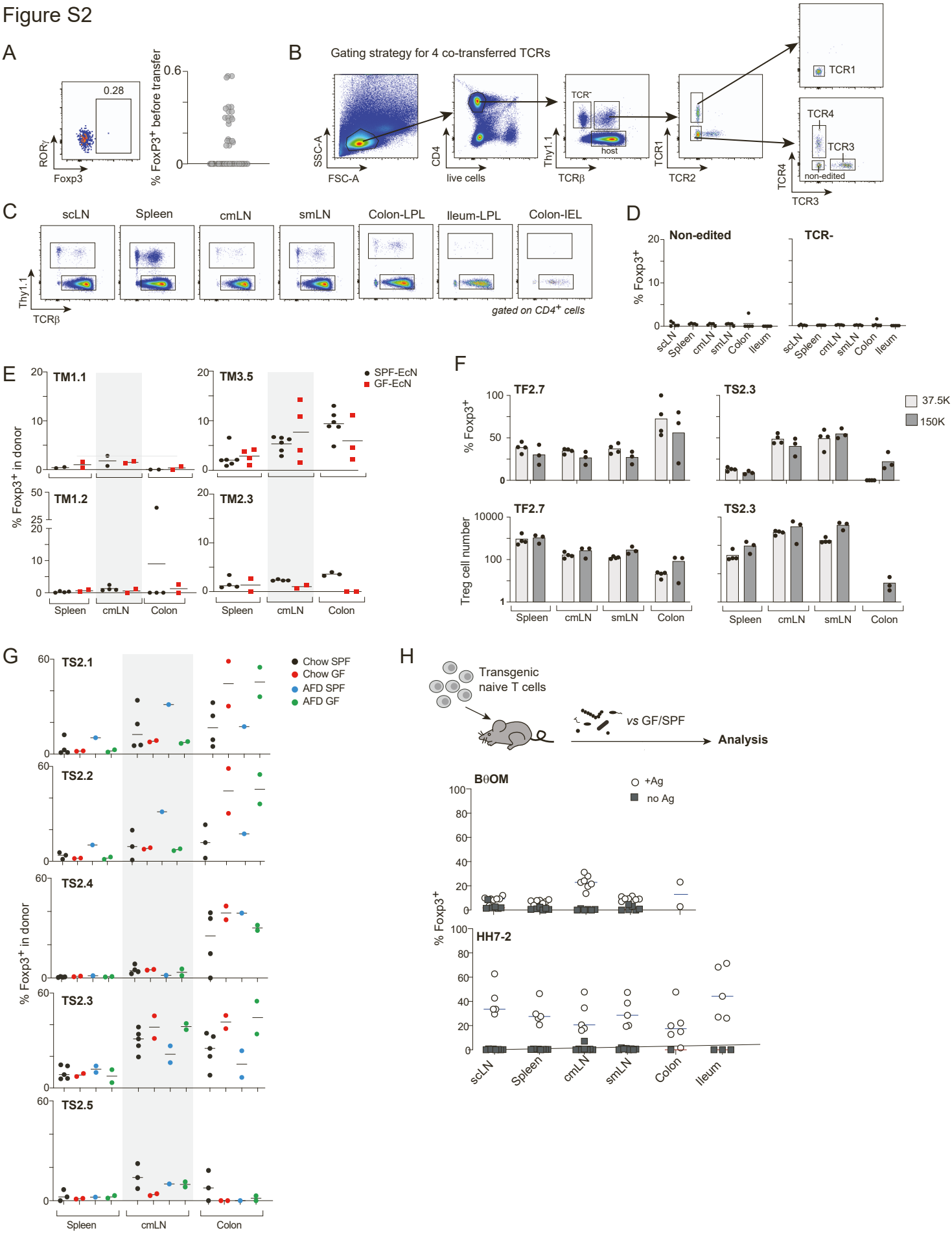
A
0.28
RORγ
Foxp3
% FoxP3+ before transfer
0.6
0
B
Gating strategy for 4 co-transferred TCRs
SSC-A
FSC-A
CD4
live cells
TCR-
Thy1.1
TCRβ
host
TCR1
TCR2
TCR4
TCR3
non-edited
C
scLN
Spleen
cmLN
smLN
Colon-LPL
Ileum-LPL
Colon-IEL
Thy1.1
TCRβ
gated on CD4+ cells
D
Non-edited
TCR-
% Foxp3+
scLN
Spleen
cmLN
smLN
Colon
Ileum
E
TM1.1
TM3.5
TM1.2
TM2.3
% Foxp3+ in donor
SPF-EcN
GF-EcN
Spleen
cmLN
Colon
F
TF2.7
TS2.3
% Foxp3+
Treg cell number
37.5K
150K
Spleen
cmLN
smLN
Colon
G
TS2.1
TS2.2
TS2.4
TS2.3
TS2.5
% Foxp3+ in donor
Chow SPF
Chow GF
AFD SPF
AFD GF
Spleen
cmLN
Colon
H
Transgenic
naive T cells
vs GF/SPF
Analysis
BθOM
HH7-2
+Ag
no Ag
% Foxp3+
scLN
Spleen
cmLN
smLN
Colon
Ileum

Figure S3

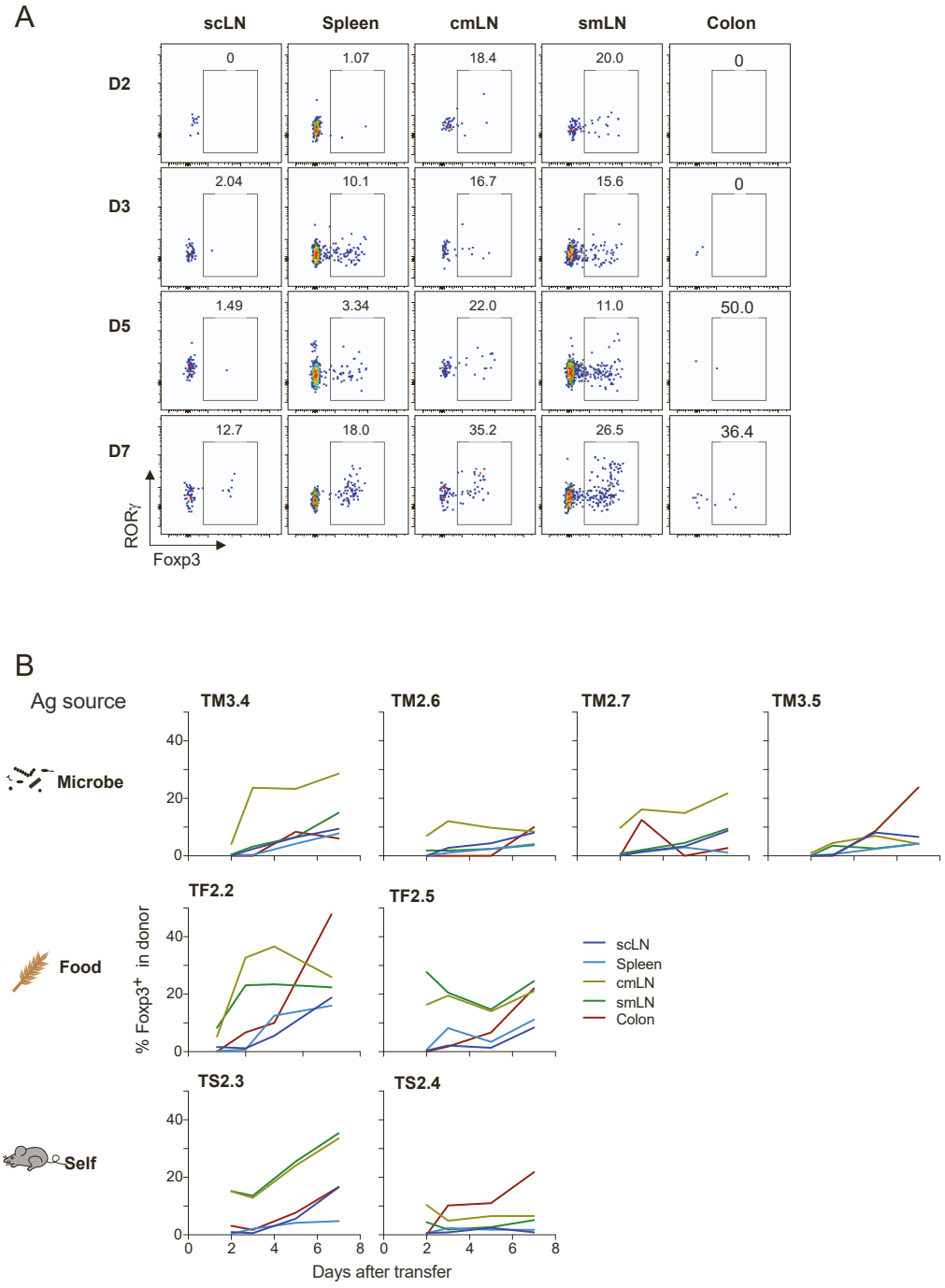
A
scLN
Spleen
cmLN
smLN
Colon
D2
D3
D5
D7
0
1.07
18.4
20.0
0
2.04
10.1
16.7
15.6
0
1.49
3.34
22.0
11.0
50.0
12.7
18.0
35.2
26.5
36.4
RORγ
Foxp3
B
Ag source
Microbe
Food
Self
TM3.4
TM2.6
TM2.7
TM3.5
TF2.2
TF2.5
TS2.3
TS2.4
% Foxp3+ in donor
Days after transfer
scLN
Spleen
cmLN
smLN
Colon

Figure S4

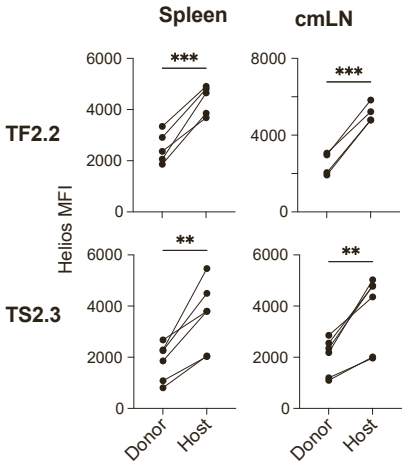
Spleen
cmLN
TF2.2
TS2.3
Helios MFI
6000
4000
2000
0
8000
***
**
Donor
Host

Fig. S5

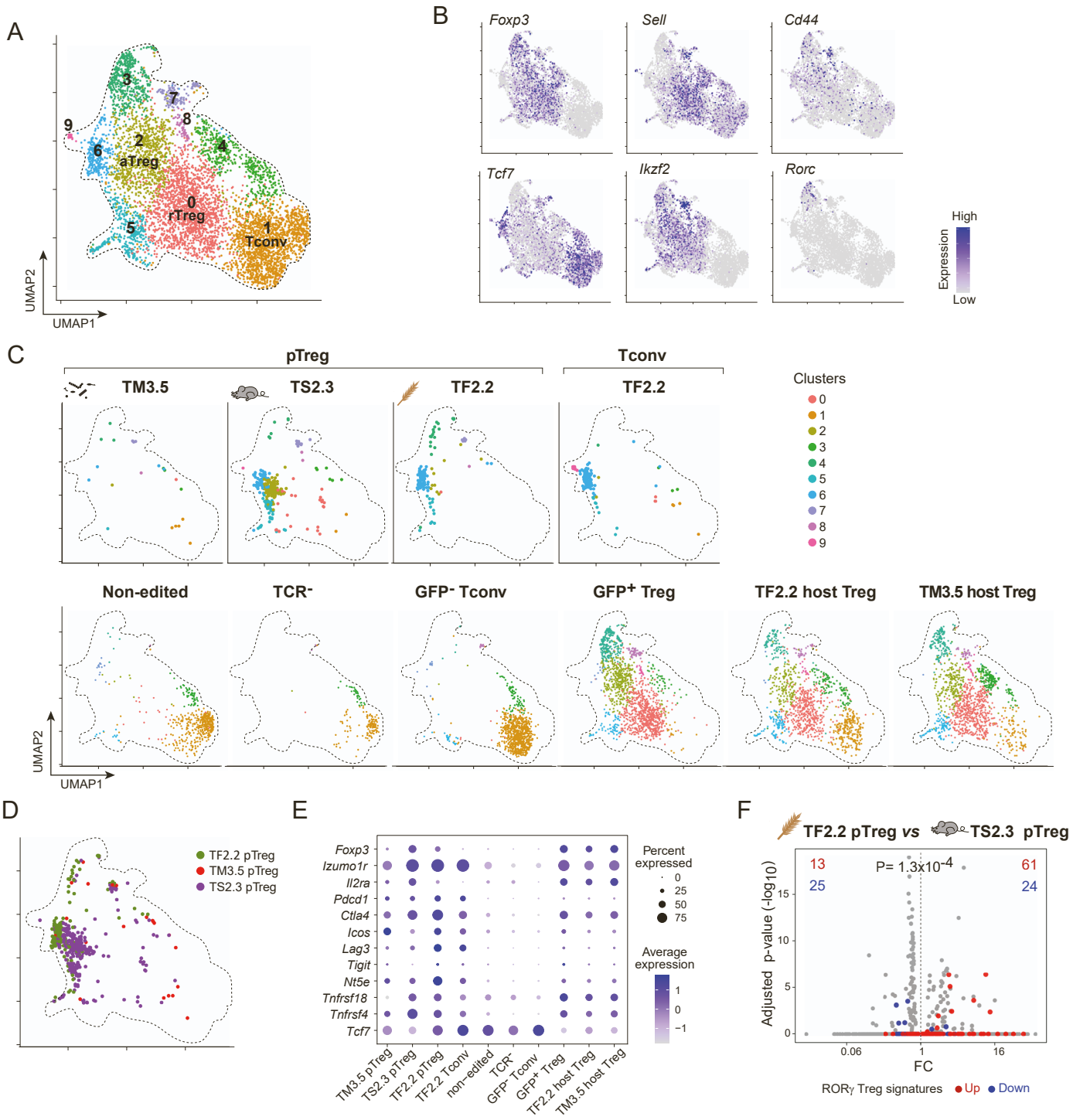
A
B
C
D
E
F
UMAP1
UMAP2
aTreg
rTreg
Tconv
Foxp3
Sell
Cd44
Tcf7
Ikzf2
Rorc
High
Low
Expression
pTreg
Tconv
TM3.5
TS2.3
TF2.2
Clusters
Non-edited
TCR-
GFP- Tconv
GFP+ Treg
TF2.2 host Treg
TM3.5 host Treg
TF2.2 pTreg
TM3.5 pTreg
TS2.3 pTreg
Izumo1r
Il2ra
Pdcd1
Ctla4
Icos
Lag3
Tigit
Nt5e
Tnfrsf18
Tnfrsf4
Percent expressed
Average expression
TF2.2 pTreg vs TS2.3 pTreg
P= 1.3x10-4
Adjusted p-value (-log10)
FC
RORγ Treg signatures
Up
Down